

# MATERIALS, TECHNOLOGIES, CONSTRUCTIONS

## **“Special purpose processes”**

Redakcja naukowa:  
dr hab. inż. Mirosław Tupaj, prof. PRz



Stalowa Wola 2019

Wydano za zgodą Rektora

O p i n i o d a w c y

prof. dr hab. inż. Grzegorz Budzik  
dr hab. inż. Andrzej Trytek, prof. PRz

R e d a k t o r n a c z e l n y

Wydawnictw Politechniki Rzeszowskiej  
prof. dr hab. Grzegorz Ostasz

R e d a k t o r W y d a n i a

dr hab. inż. Mirosław Tupaj, prof. PRz

O p r a c o w a n i e m a t r y c y o k ł a d k i

dr inż. Joanna Zielińska-Szwajka  
mgr inż. Sylwia Sikorska-Czupryna

*materials, technologies,  
constructions, testing*

© Copyright by Oficyna Wydawnicza Politechniki Rzeszowskiej  
Rzeszów 2019

ISBN 978-83-7934-358-4

Ark. wyd. 5,10, ark. druk. 5,50  
Oficyna Wydawnicza Politechniki Rzeszowskiej  
al. Powstańców Warszawy 12, 35-959 Rzeszów  
<https://oficyna.prz.edu.pl>  
Zam. nr 102/19

## Table of Contents

Chapter 1. SELECTED LASER CUTTING PROBLEMS IN THE CONTEXT OF THE „INDUSTRY 4.0” CONCEPT Tomasz WIĘCEK, Barbara CIECIŃSKA, Leszek PYZIAK .....	5
Chapter 2. INFLUENCE OF THE CUTTING TOOL PROPERTIES ON THE TREATMENT SURFACE QUALITY IN THE HEAT RESISTANT STEEL BROACHING Olha DVIRNA .....	27
Chapter 3. POSSIBILITIES OF IMPROVE THE PRODUCTIVITY OF OPERATIVE PROGRAMS Józef BRZĘCZEK .....	39
Chapter 4. COMPARISON OF THE PROPERTIES OF TITANIUM CARBIDE IN TITANIUM MATRIX NANOCOMPOSITES MANUFACTURED BY SLM AND SPS TECHNIQUE Paweł FIGIEL, Anna BIEDUNKIEWICZ, Witold BIEDUNKIEWICZ, Dariusz GRZESIAK, Dariusz GRABIEC .....	57
Chapter 5. PEEK AND PEEK-BASED COATINGS FOR IMPROVEMENT OF THE Ti-6Al-4V ALLOY'S TRIBOLOGICAL PROPERTIES Aleksandra KRUK, Sławomir ZIMOWSKI, Tomasz MOSKALEWICZ.....	71



## Chapter 1.

**Tomasz WIĘCEK<sup>1\*</sup>**  
**Barbara CIECIŃSKA<sup>2</sup>**  
**Leszek PYZIAK<sup>1</sup>**

# SELECTED LASER CUTTING PROBLEMS IN THE CONTEXT OF THE „INDUSTRY 4.0” CONCEPT

### Abstract

The chapter presents the characteristics of laser techniques used in modern industry. Machining capabilities in the context of the construction materials used, the obtained results and the advantages compared to conventional operations have been described in this work.

Particular attention was paid to the development trends and production needs in the currently observed industrial revolution the Industry 4.0. In accordance with the requirements of the Industry 4.0, necessary comprehensive automation, digitization of production, the need for a flexible approach in the production of diversified products on a massive scale, lasers in various configurations are an interesting alternative to existing solutions.

Particular emphasis was placed on laser cutting operations of selected plastics. Problems occurring in machining were presented; it was contrasted with the effects of laser cutting. An experiment for selected plastics was carried out, and the method of determining the optimal processing parameters was characterized.

A number of examples justifying the need to select parameters for plastics, especially flammable, have been presented, due to the danger of ignition. The advantages of laser machining in the context of the Industry 4.0 revolution have been demonstrated.

### Key words:

Laser, plastics, cutting, Industry 4.0

---

<sup>1</sup> Department of Applied Optics, Rzeszów University of Technology, Powstańców Warszawy 12, 35-959 Rzeszów, Poland

<sup>2</sup> Department of Manufacturing Processes and Production Engineering, Rzeszów University of Technology, Powstańców Warszawy 12, 35-959 Rzeszów, Poland

\* ftkwiece@prz.edu.pl

## **1. Introduction**

### **1.1. The concept of the Industry 4.0 and the place of laser technology**

The Industry 4.0 is a description of the changes that modern industry is experiencing at the present time. The concept of the Industry 4.0 assumes a change in manufacturing processes focusing on mass production of individualized products, compared to previous manufacturing processes focused on the mass production of identical products. This requires an extraordinary, flexible design of production lines in which individual technological processes can be carried out. This flexibility, on an unprecedented scale, is possible thanks to comprehensive computerization, automation and robotization of processes. Due to the need to meet various customers' orders in a short time, a comprehensive digitization of processes in the company is necessary.

The Industry 4.0 concept assumes that the basis of such an approach is the integration of systems and the creation of a network of information flow not only between people, but also between people and machines. The huge amount of data (Big Data) used for this purpose, collected in a data cloud, should be supported by decision-making systems based on elements of artificial intelligence [1]. Then, the implementation of various technological operations and production management in a broad sense require a minimum of time.

For the vision of the Industry 4.0 to be fulfilled, all parts of the production line should be compatible with each other. Many manufacturers, to meet these requirements, offer enterprises both machine tools and other components, e.g. sorting devices, conveyors, interchangeable tables with complete equipment, etc. process execution elements with tailored software [2]. Then it can be said that the supplier offers the entire factory (fig. 1.1).



a)



b)

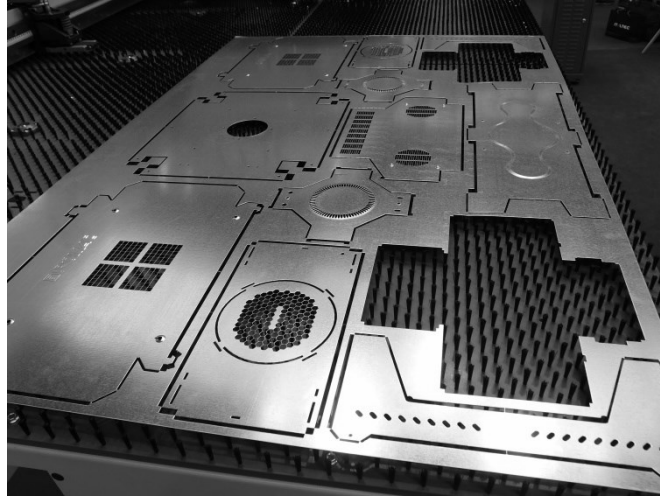


c)

Fig. 1.1. Examples of comprehensive solutions for the Industry 4.0: a) planning and real-time control of the implementation of cutting operations, b) pallets for depositing finished products, c) bending station with a robotic exchanger of fittings [B. Ciecńska]

The assumption of the Industry 4.0 is to create a logical sequence of technological operations that enables immediate retooling and matching of machining parameters to the order. Laser technology is a perfect match to this idea. The variety of laser applications described earlier gives a wide range of possibilities to build integrated production lines. Laser heads placed in machining centres allow for combined machining, e.g. punching, drilling, welding, etc. with simultaneous reduction of execution time [3]. Often lasers replace conventional workstations, e.g. for cutting, engraving, hardening and others. In addition, laser measuring systems, various types of sensors, code readers complement machining operations with product identification features, measurements or marking (fig. 1.2).





a)



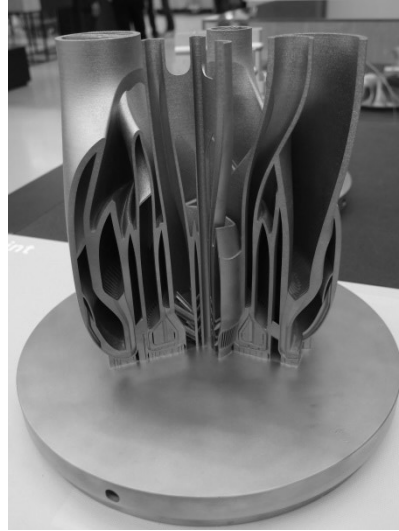
b)

Fig. 1.2. The variety of possibilities of using lasers in the production line: a) cutting various products from one sheet of metal, b) combining cutting and bending of sheet metal in one production socket [B. Ciecńska]

An additional advantage of laser technology is the ease of changing the parameters of processing (loading an appropriate file), cleanliness at workstations, safety, benefits in relation to postulates without waste or low-waste production, energy-saving, lack of chemicals, the ability to process products of virtually unlimited shape (3D printing technology) or size (fig. 1.3).



a)



b)



c)

Fig. 1.3. Possibilities of laser technology: a) cutting in combination with bending of the product with a mass of 300 kg and a wall thickness of 35 mm, b) model elements made with the laser sintering technique, c) elements welded with a laser [B. Ciecńska]

### 1.2. The use of lasers in machining of construction materials

There are many known methods, such as moulding (casting, powder metallurgy), plastic forming (including forging, rolling, extrusion, stamping) and subtractive manufacturing (abrasive machining, machine cutting, erosive machining) using well known and available technological devices and machines.

The trend in the development of manufacturing technology observed in recent years is the increasingly widespread use of laser technology in various areas.

Laser treatment in connection with the most commonly obtained effects can be divided into two basic groups: remelting and non-melting techniques [4].

In order to modify the surface layer properties of a laser beam, a variety of methods are used, such as ***strengthening transformation, partial melting of the surface layer*** – during which the laser heats a thin layer of the treated surface (e.g. surface hardening). As a result of the treatment, a finely dispersed and more homogeneous structure is obtained, although the surface roughness deteriorates. However, the exploitation properties - tribological, fatigue and anti-corrosion improve. In this way, elements made of many different materials can be modified: grey cast iron, tool steels, including high-speed ones, stainless, bearing, carbon and low-alloy steels as well as aluminium alloys or pure titanium [4, 5].

Another type of treatment is glazing. Its purpose is to obtain an amorphous structure in the surface layer. This is a rather difficult treatment, as not all alloys tend to amorphise. At high cooling rates, the viscosity of the liquid metal in some alloys increases so that the alloy does not crystallize. It solidifies in an unstructured way, creating an amorphous alloy with the features of glass in the mass. Glazing is successful in non-eutectic alloys based on tellurium matrix from Ag, Ga, Cu, In; on lead and tin matrices (e.g., Pb-Sn, Pb-Au, Sn-Cu et al.) and many others. Amorphous alloys are characterized by considerable strength and hardness, while maintaining their ductility, although their strength at low temperatures decreases. They are characterized by high resistance to corrosion, and some of them exhibit special magnetic properties [4].

With the partial melting of the surface layer, ***laser densification*** also involves melting the material down to a certain depth in order to obtain a material of higher density. Most often as a result of densification, porosity, surface defects such as scratches, delamination, etc. are removed. The densified surfaces of the products are characterized by higher hardness, smoothness, higher resistance to tribological and fatigue wear and are more resistant to corrosion. Densification is used to seal surfaces, e.g. steel with carbides, thermal spray coatings or galvanic coatings [4].

Similarly, comparing the processing parameters, ***laser smoothing*** is performed. The material structure has the same phase and structural changes, but the main objective is to reduce surface roughness and change the shape of the uneven profile. Sometimes, the improvement of smoothness is obtained with the addition of additives to the molten zone of the material (the so-called pool), affecting the behaviour of the material (volume of swirls, speed and direction of circulation), but then it is already smoothing alloying [4].

Another way of processing materials is ***the introduction of alloying elements***, which takes place by melting the material and material of the object then the melted materials are mixed. The passage of the laser beam also triggers the self-hardening effect of the substrate material in the vicinity of the newly formed alloy. The products manufactured in this way are characterized by a top layer

with increased fatigue strength, better tribological properties, anti-corrosion properties and lower roughness. Non-metals (C, N, Si, B), metals (among others Co, Cr, Sn, Mn, Nb, W, Ta) and carbides of refractory metals are used for alloying, while steels and cast iron are used for laser alloying. Single elements are melted to improve heat resistance and creep resistance, anti-corrosion and anti-abrasion properties [6].

Laser energy is also used to regenerate used elements in the way of **pad welding(rebuilding)**. Then, the melted metal is used to fill gaps, cracks, chipping and to reconstruct worn surfaces. In some cases, apart from reconstructing the shape and restoring lost properties, these properties can be improved (refinement). This is possible by applying a material with a modified composition. In this way, the surface layer is formed with greater resistance to corrosion, erosion, abrasion, cavitation, increased heat resistance and creep resistance. Among others, steel, cobalt alloys, titanium alloys, aluminium alloys are pad welded [7-10].

For the treatment of selected areas of the surface, lasers are used for annealing or tempering as well as hardening.

The main purpose of **annealing** is to homogenize the structure; structural defects are reduced, in some cases the density may increase. Due to the fact that the laser spot is not large, laser annealing is used for local heating, and thus for local reduction of hardness, plasticity, and subsequent deformation of these places or increasing fatigue strength [4].

**Laser tempering** allows heating to a certain temperature and cooling, and is used to improve ductility and to reduce brittleness. Local impact of the beam offers a number of advantages: phase and structural changes occur in a similar way as during the furnace treatment, but the carbides are more fine-grained, the material has higher hardness, strength and impact resistance. These properties can be adjusted by changing the operating parameters of the laser. In addition, stresses, e.g. hardening are removed locally [4].

Laser beam also allows **hardening**. Due to much higher heating and cooling speeds, it runs at a higher temperature than classical hardening. In laser-hardened materials, fatigue strength, impact strength, ductility, corrosion resistance and abrasive wear increase, uniform distribution of hardness and better surface smoothness are obtained, although the nature of changes depends on the type of the material and procedures prior to the treatment [6, 11].

In turn, the use of the phenomenon of ablation, i.e. evaporation or laser etching, allows **cleaning** of the surfaces of various types of materials. As a result of the impact of the impulse, the energy is absorbed, the surface layer is partially melted, and the material is rapidly evaporated from the molten zone and ejected in the form of plasma - fragments of material particles and the products of reaction [6, 12]. In this way, various organic and inorganic multiple layers can be removed from concrete and metal objects covered with varnish. This method has

been used in gluing technology, where it is possible to degrease and clean the surface before applying the glue, but also, for example in the renovation of works of art, where it is sometimes successfully removed from centuries-old layers without damaging the original material [13, 14].

The above-mentioned ways of using energy emitted by lasers do not exhaust their application areas. Among other machining methods, the production of thin and hard coatings can be distinguished, including coatings with special properties [4, 12] or intensively developed incremental growth in recent years, including spatial adhesion of powders with 3D printing (three-dimensional printing), selective laser sintering (SLS) and others [5, 15].

### **1.2. Another way of using the energy of the beam – laser cutting**

Lasers successfully replace existing methods of material processing, such as cutting. Cutting and cutting of elements occurs as a result of local melting and evaporation of the material by means of a laser beam with a specific energy. Laser cutting technology is distinguished by the following varieties:

- cutting thin or thick layers of material without damaging the substrate to which they are applied - used in electronics,
- shallow cutting of materials, e.g. ceramics or semiconductors (application as above),
- cutting of metals and other materials with a greater thickness, used in the production of various products.

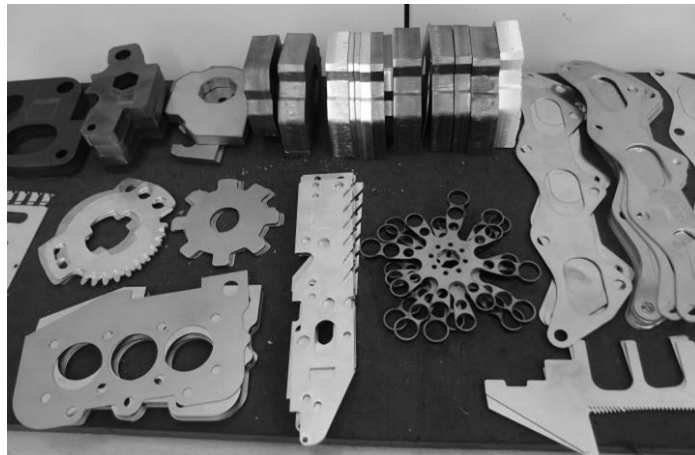
CO<sub>2</sub> lasers with continuous and high-power operation are used for cutting materials. They allow the user to cut elements of steel, titanium and its alloys, tantalum, zirconium and its alloys, nickel alloys, aluminium and non-metals - such as wood, plastics, fabrics, leather, etc.

Laser cutting is characterized by high cutting speed, easy cutting out of complicated shapes, relatively good cutting edge quality, small size of thermal impact zone in the material being cut and non-contact action [16].

Cutting operations, depending on the material being processed, may proceed at different speeds, while the parameters of the laser beam are important due to the thickness of the material being cut, the width of the incision and the size of the heat-affected zone. In many cases, cutting should take place in an atmosphere of active gas - oxygen or neutral - argon or nitrogen. The active atmosphere is most often used for metalworking, gas significantly increases the absorption of laser radiation due to the oxidation of the surface of the cut metal, increasing the surface temperature at the processing site by extracting heat in the oxidation reaction, removing vapour and fragments of molten metal from the processing site and facilitating access for the laser beam to the cutting gap. The use of oxygen allows increasing the cutting speed by approx. 40%. However, it can degrade the quality of the edges after cutting and increase the size of the gap. In any case, the laser parameters and oxygen flow should be selected depending on the type of the material to avoid these difficulties. Also, the material should not be cooled

excessively by unnecessarily excessive gas flow. Some materials, such as gold, must be prepared for cutting and are only processed as thin layers applied to the dielectric substrate (to avoid burning the material). The inert gas also increases the efficiency of cutting. This is due to the removal of melted or evaporating material from the processing site, the facilitation and displacement of the beam access into the incision, and the prevention of burning of the upper edges of the incision due to gas cooling. In an inert gas atmosphere it is possible to cut elements from metals, wood, plywood, cardboard, paper, asbestos, textiles, rubber, plastics, ceramics and many more. In each case, the cutting operation requires control of the choice of process parameters: cutting speed, laser beam power, degree of beam focus, gas stream size as depth, where width and shape of the incision depend on one another [16].

Sometimes, gas is not needed, e.g. in modern production solutions using marking lasers, low power (20-35 W), it is possible to cut materials (an example can be cutting aluminium tiles up to 1,5 mm thick). Another method is the use of fibre and diode lasers (especially high power - the so-called multi kW) for cutting elements of considerable thickness - above 10 mm - in this way cutting can take place in an atmosphere of oxygen [17] (fig. 1.4).



a)



b)

Fig. 1.4. Photographs of laser-cut objects: a) various materials of products, b) elements of considerable thickness [B. Ciecńska]

In the context of the issue of cutting plastic further discussed in the paper, the use of a laser beam for cutting materials can be beneficial in many respects. Plastics are subjected not only to plastic working but also to machining. Then, laser cutting allows avoiding difficulties, especially with poor quality of the resulting surface. The quality of the product is particularly dependent on the process of chip formation. When machining polymers, different chips may be formed: continuous, discontinuous, plastically deformed, etc. Continuous chips may hinder the processing due to the tendency to upset, stick the object or tool, impair not only the visibility of the treatment zone, but they also reduce work safety.

The layering chips can increase the cutting forces and increase the temperature, which facilitates polymer chipping. Similarly, discontinuous chips - detached (chipped) deteriorate the surface of the treated surface. A special case of discontinuous chips is fine dust, also affecting faster tool wear [18].

## 2. Laser cutting of plastics

Plastics are a group of modern materials used in various fields of production. The characteristic properties of plastics mean that they are not only substitutes for metal materials, but they also allow to design completely new products with surprising shapes and useful properties. When compared with metals, they have a number of advantages, such as low density, vibrations dampening, electrical insulation or regulated electrical conductivity, chemical resistance, corrosion resistance and the ability to modify properties due to a variety of additives [19].

An alternative way of cutting plastics for the previously presented mechanical cutting (machining) can be cutting with a laser beam, which in recent years has

become more and more popular. Laser cutting is a direct action of a laser beam on the selected area of the material. In order to heat the material in the area of the cutting gap to the melting or evaporation temperature, the laser beam must provide the required energy [20, 21]. In most cases, the material is immediately evaporated and the heat affected zone is very small.

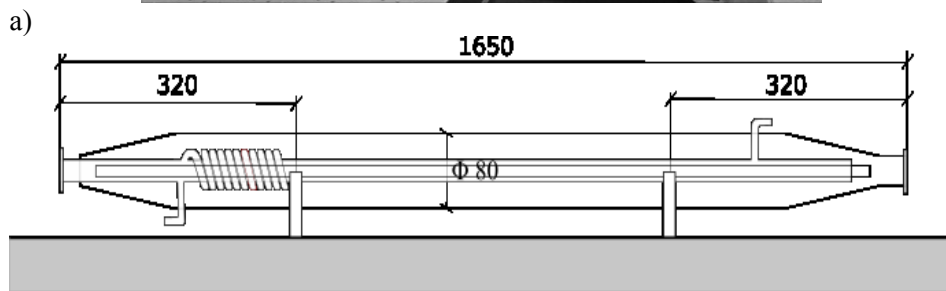
From the point of view of the technological process of plastics processing, lasers have become popular due to the advantages of the process: reproducibility of settings, susceptibility to automation, controllability, durability of a laser beam as a tool. In addition, they are a source of moderate noise; there are less harmful factors as well as waste and material losses. They do not show any defects typical of machining. Laser treatment can be used for both homogeneous and layered materials (laminates). The laser causes low internal stresses and allows to cut complicated shapes of the elements, thus objects do not usually require finishing [22, 23]. Technological solutions are also interesting - laser punching machines that work with robots, with tilting heads or systems enabling the beam division and simultaneous multi-station machining are already produced [24, 25]. For this reason, laser cutting is used in many industries, e.g. automotive, aerospace or machine-building [23].

### **2.1. Experimental research results of laser cutting of acrylic**

Methyl polymethacrylate is commonly known as acrylic and is the only commonly used material that is laser-cut by evaporation. Acrylic is boiled to give off a pair of methyl methacrylate, making it possible to conclude that there is a minimal amount of chemical degradation, and the process is getting closer to a purely physical change of phase from solid to liquid and then to steam. The cutting edge is of extremely high quality and exceeds the quality of the edge polished by flame. In the conducted experimental studies, a CO<sub>2</sub> laser with a single-mode beam was used (fig. 1.5).

The material was static during cutting and the laser beam changed its position and was computer-controlled. In order to increase the power density, a lens with a lens made of ZnSe with a focal length  $f = 6,35$  mm was used.





b)  
 Fig. 1.5. Laser plotter 150W (a) [B. Ciecńska] and a diagram of a CO<sub>2</sub> laser tube (b) [L. Pyziak]

In order to determine the optimal parameters of acrylic cutting, a series of cuts was made at different beam speeds (fig. 1.6 and tab. 1.1) in accordance with the beam diagram shown in fig. 1.7.

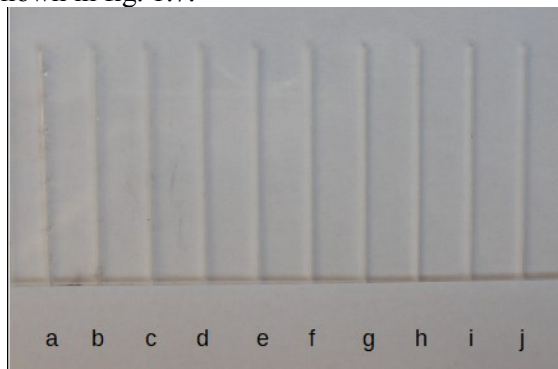


Fig. 1.6. Laser cutting of acrylic [T. Więcek]

Table 1.1. The options of speed - laser cutting of acrylic

	Options of cutting									
Symbol	a	b	c	d	e	f	g	h	i	j
Speed [mm/s]	5	10	15	20	25	30	35	40	45	50

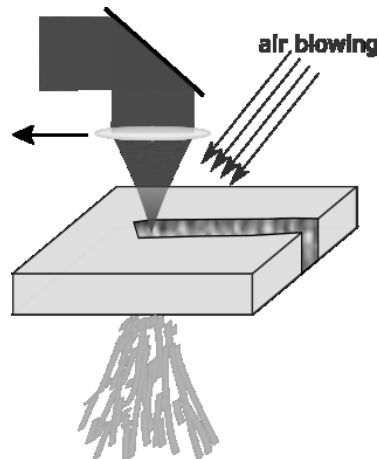
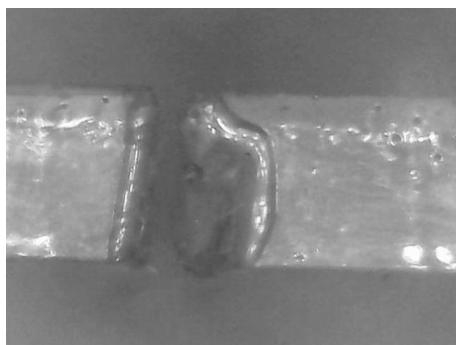
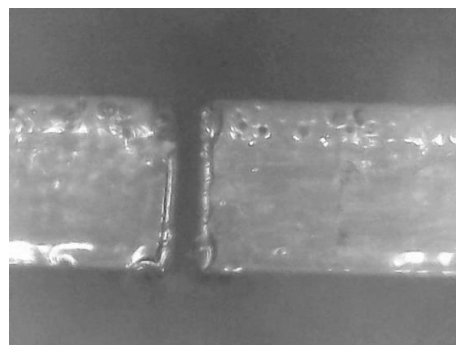


Fig. 1.7. Focusing the laser beam during cutting [L. Pyziak]

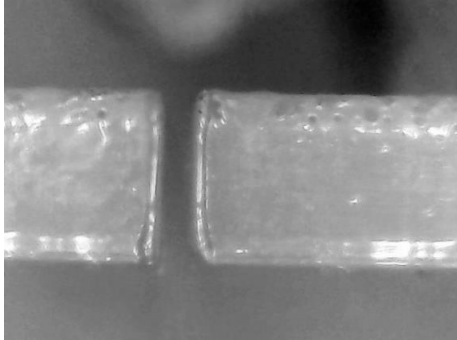
As a result of the experiment, the results shown in fig. 1.8 were obtained. Not all cuttings visible in the photographs were characterized by satisfactory edge quality. It has been found that in selected cases it is possible that the material will not be cut at all (e.g. fig. 1.8i), which may be due to too high cutting speed (in the range of speeds assumed in the experiment).



a) 5 mm/s (the worst result)



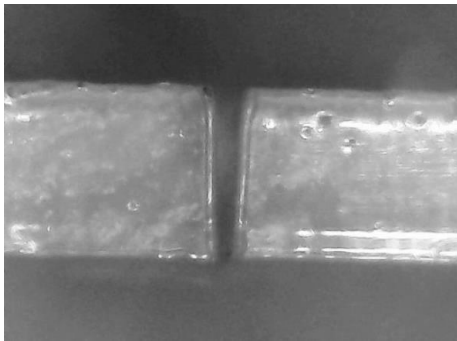
b) 10 mm/s



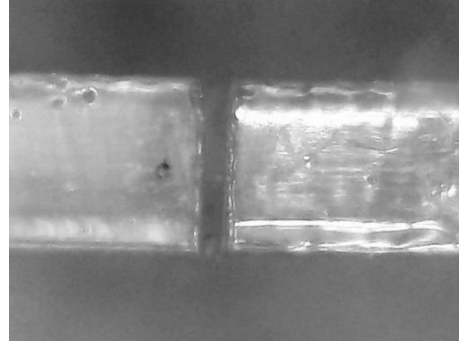
c) 15 mm/s



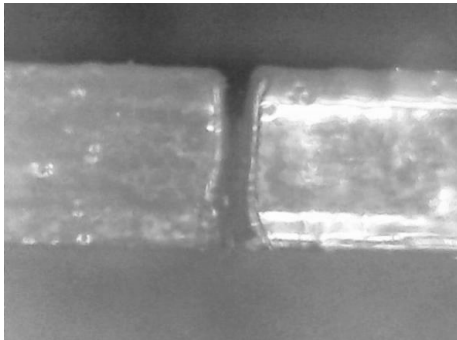
d) 20 mm/s



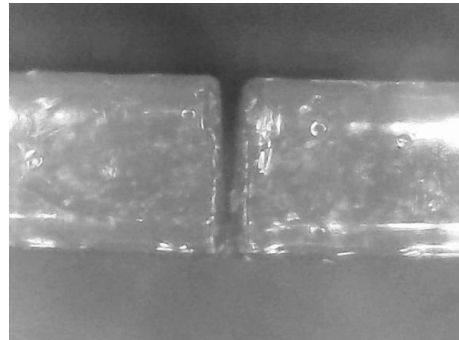
e) 25 mm/s



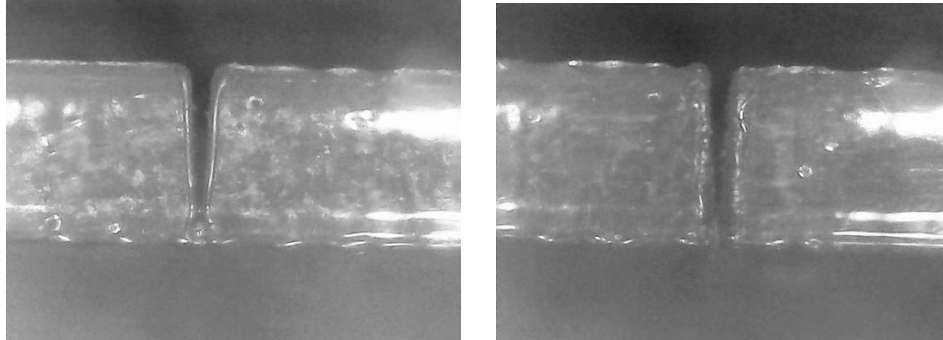
f) 30 mm/s (optimal result)



g) 35 mm/s



h) 40 mm/s



i) 45 mm/s (no cut)

j) 50 mm/s (no cut)

Fig. 1.8. The results of laser cutting of acrylic: a) – j) with different speed of cutting [T. Więcek]

As a result of observing the cuts, it was found that the cutting speed should be individually selected for the material being processed. For this reason, in order to determine the dependence convenient to determine the optimal speed, calculations were made in which the acrylic thickness was assumed = 2 mm, the maximum cutting speed = 30 mm/s = 1,8 m/min (experimentally determined, fig. 1.8f). The experiment has shown that at higher cutting speed the material would over-melt excessively (fig. 1.8g, h) until there was no cut (fig. 1.8i and j).

Substituting values for the equation [26]:

$$V = P \cdot Q \cdot t^{-1,35} \quad (1)$$

where:

$V$  - maximum cutting speed (1,8 m/min),

$P$  - laser power (150W),

$t$  - material thickness (2 mm),

$Q$  - fixed, calculated value, characteristic of the material,

the following result was obtained:

$$Q = V / (P \cdot t^{-1,35}) \quad (2)$$

Then

$$Q = 1,8 / (150 \cdot 2^{-1,35})$$

$$Q = 0,031.$$

By entering this value into the equation, the cutting speed was estimated at any laser power and any acrylic thickness:

$$V = P \cdot 0,031 \cdot t^{-1,35}$$

Therefore, for example, with a power of 75W and acrylic thickness of 4 mm, the maximum cutting speed should be:

$$V = 75 \cdot 0,031 \cdot 4^{-1,35}$$

$$V = 0,35 \text{ m/min.}$$

## 2.2. Laser cutting of polypropylene

Due to the fact that laser cutting is a direct effect of a laser beam on the area of the cutting gap and that there is a risk of igniting the material, the process of cutting polypropylene and propylene with 30% addition of talc was investigated. A laser presented in point 2.1. was used for this experiment. As in the case of acrylic, a series of 5 mm thick polypropylene cuts was made at different cutting power and speed. In the cutting process, a blow of air was used to protect the lens from the pairs of the workpiece (particularly as soot may appear in the case of polypropylene. This phenomenon was not observed in acrylic cutting). Due to the justified risk of material ignition, proper selection of processing parameters is of particular importance. The results of cutting propylene with talc are shown in fig. 1.9 and fig. 1.10, although the cutting was carried out from the highest speed, gradually reducing it. Fig. 1.11-1.16 show the results of cutting both of the propylene varieties.



Fig. 1.9. Polypropylene Moplen HP500N laser cutting with talc - side view, composite ignites, gaps on the left side for 150W laser power, on the right side for the power of 113W

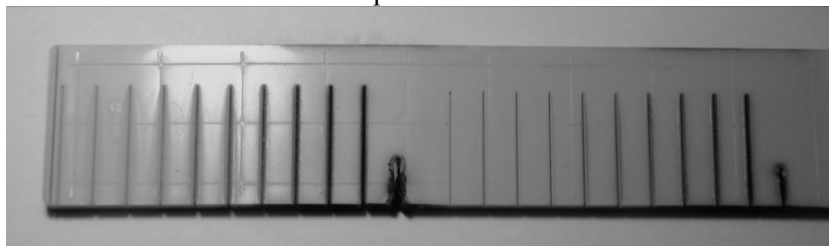


Fig. 1.10. Moplen HP500N polypropylene laser cutting with talc - top view, left-hand gaps for 150W laser power, on the right side for the power of 113W

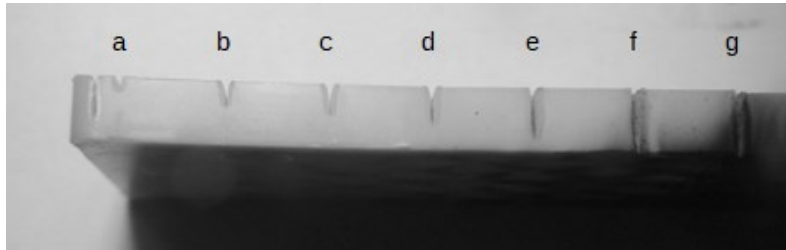


Fig. 1.11. Laser power 150W, cutting the composite at speeds of: a) 50, b) 25, c) 20, d) 15, e) 10, f) 8, g) 6 mm/s

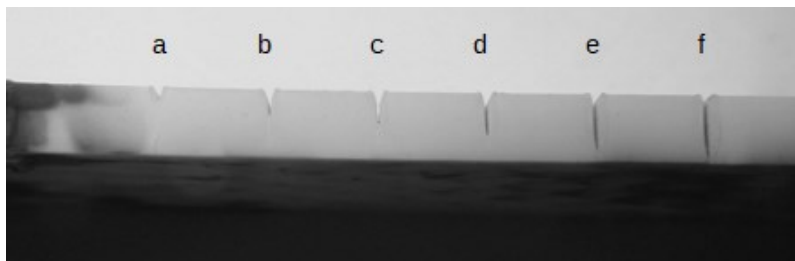


Fig. 1.12. Laser power of 113W, composite cutting at speeds of: a) 50, b) 25, c) 20, d) 15, e) 10, f) 8 mm/s

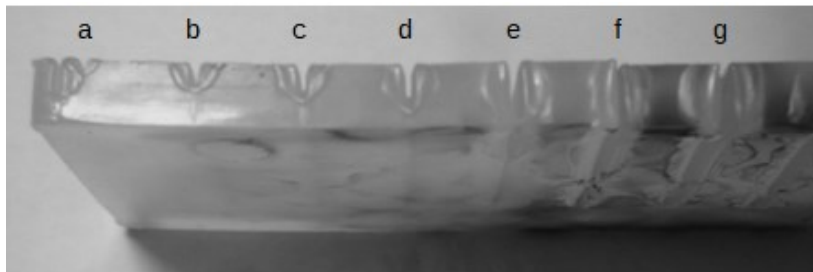


Fig. 1.13. Laser power of 150W, cutting of polypropylene at speeds of: a) 50, b) 25, c) 20, d) 15, e) 10, f) 8, g) 6 mm/s

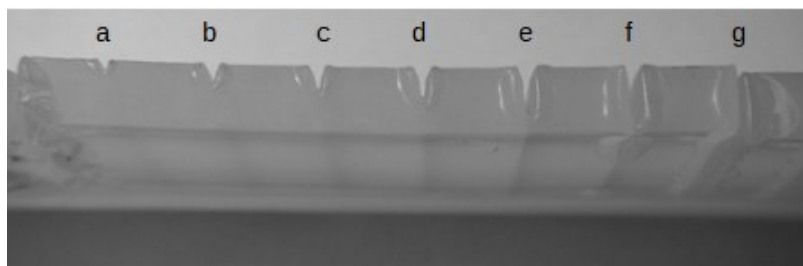


Fig. 1.14. Laser power of 113W, cutting of polypropylene at speeds of: a) 50, b) 25, c) 20, d) 15, e) 10, f) 8, g) 6 mm/s

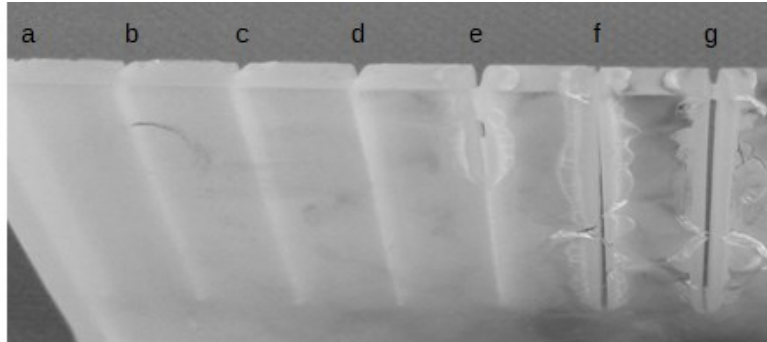


Fig. 1.15. Laser power of 150W, cutting of polypropylene at a) 50, b) 25, c) 20, d) 15, e) 10, f) 8, g) 6 mm/s (from left), bottom view

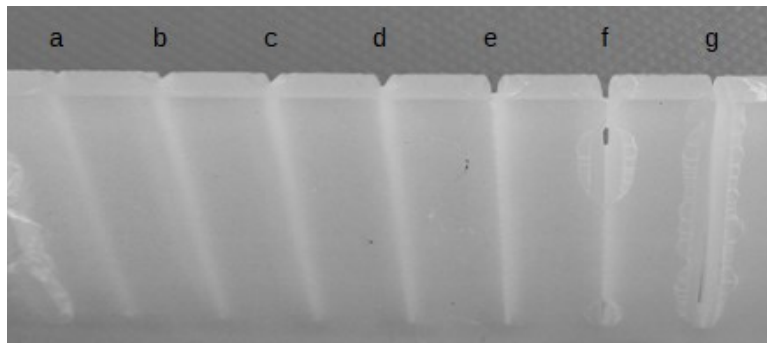


Fig. 1.16. Laser power of 113W, cutting of polypropylene at a) 50, b) 25, c) 20, d) 15, e) 10, f) 8, g) 6 mm/s (from left), bottom view

Experimental studies show a change in the depth of the cut in a speed function for different laser beam power (fig. 1.11-1.16). It has been found that with the increase of the laser beam power it is possible to increase the cutting speed.

In addition, it can be stated that only for low power density there is no material combustion process and no blowing is required (fig. 1.16). In the case of acrylic cutting, the risk of burning did not occur. The more the power, the bigger increase of the cutting speed is obtained which is noticeable on the case of polypropylene. The laser of power of 113W gives possibility of the machining with the speed of 8 mm/s, and the laser of power of 150W – speed of 10 mm/s. These values are consistent with theoretical relations [26]. It is difficult to assess the cutting quality for gaps with soot. In this case, the cutting process should be repeated with an inert gas blow. Taking into account the cutting parameters, the formation of a thermal zone on the edge of the gap is easily noticeable. The fluid material can close the gap and in this case the gas flow should be increased. This case was observed in fig. 1.15 and fig. 1.16 (both f and g).

### **3. Conclusions**

Due to the greater availability of laser devices, it is possible to use a much larger group of technological operations in today's enterprises dedicated to a wide range of construction materials. These operations can be managed in a modern, automated way as they meet not only the demands of production Just in Time (JiT) but they also meet the demands of certain savings in manufacturing processes (according to the concept of Lean Manufacturing). The use of lasers allows for a cleaner, with a reduced amount of waste or non-waste production giving the opportunity to produce high quality products.

In some cases, the use of laser allows to eliminate commonly used chemicals, often criticized as a harmful to the environment. However, it is important to remember to use industrial filters due to the risk of poisoning and irritating fumes during the plastics processing. In the investigated case of plastic processing, laser cutting has also made it possible to avoid many problems typical of machining – like spalling of the surface and rough edge.

A prerequisite for a safe and efficient laser treatment is proper adjustment of the machining parameters to the grade and thickness of the material. In the analyzed cutting operations, dependence of the cutting speed and laser beam power was found, with the edge quality. In extreme cases, where the speed was too high, the material was not separated. In turn, too low speed of cutting gave a torn and rough edge of the cut. In spite of these inconveniences, laser cutting was much faster than the conventional one, and the narrower gap was created (advantageous feature due to material saving).

When comparing the materials studied, one should remember about their features, which in the case of methods with the use of concentrated energy sources may be important not only due to the quality of cutting, but also to safety. In the case of polypropylene cutting, it was determined that in a certain range of processing parameters, the combustion process takes place and it is necessary to use an inert gas blow. The gas flow rate must in turn be adapted to the melting material so that the resulting gap is not sealed during cooling (which means no cut). The above problems did not appear at all when cutting acrylic.

In conclusion, despite the need to optimize the cutting process and a careful analysis of the effects of machining of various materials, the laser cutting process is easy to use in production conditions. Due to rather uncomplicated calculations, it is possible to develop a technological guide which simplifies the design of the technological process substantially. The data can be stored in an electronic form, the laser was computer controlled, which distinguishes this technique in the context of the Industry 4.0 concept.



## References

- [1] Stadnicka D., Zielecki W., Sęp J. (2017). Koncepcja przemysł 4.0 – ocena możliwości wdrożenia na przykładzie wybranego przedsiębiorstwa. Konferencja Innowacje w Zarządzaniu i Inżynierii Produkcji, Zakopane, [http://www.ptzp.org.pl/files/konferencje/kzz/artyk\\_pdf\\_2017/T1/t1\\_472.pdf](http://www.ptzp.org.pl/files/konferencje/kzz/artyk_pdf_2017/T1/t1_472.pdf)
- [2] Industry 4.0: Benefit From Opportunities. Today. Tomorrow. Laser Technik Journal, 5/2017, pp. 12-14.
- [3] Maszyna laserowa z dodatkowymi funkcjami. TruMatic 1000 fiber. Materiały TRUMPF Polska
- [4] Burakowski T., Wierzchoń T. (1995). Inżynieria powierzchni metali. WNT, Warszawa
- [5] Oczó K., Kawalec A. (2012). Kształtowanie metali lekkich. PWN, Warszawa
- [6] Dobrzański L.A., Dobrzańska-Danikiewicz A.D. (3.05.2019). Obróbka powierzchni materiałów inżynierskich. <http://www.openaccesslibrary.com/vol05/5.pdf>
- [7] [http://www.pg.gda.pl/mech/kim/Skrypt/Inz\\_pow\\_roz5.pdf](http://www.pg.gda.pl/mech/kim/Skrypt/Inz_pow_roz5.pdf) (2.05.2019)
- [8] <http://www.e-autonaprawa.pl/artykuly/2240/technologie-napawania.html> (2.05.2019)
- [9] <http://www.megamold.pl/index.php?id=2> (2.05.2019)
- [10] Blicharski M. (2009): Inżynieria powierzchni. WNT, Warszawa
- [11] Radziejewska J. (2011). Laserowa modyfikacja warstwy wierzchniej wspomagana nagniataniem. Instytut Podstawowych Problemów Techniki PAN, Warszawa
- [12] Burakowski T., Marczak J., Napadłek W. (2006). Istota ablacyjnego czyszczenia laserowego materiałów. Prace Instytutu Elektrotechniki WAT, z. 228, Warszawa
- [13] Ciecińska B. (2016). Laser beam surface pretreatment for the adhesive bond strength improvement. Strength of Materials, Vol. 48, No4, pp. 561-565
- [14] Marczak J. (2004). Analiza i usuwanie nawarstwień obcych z różnych materiałów metodą ablacji laserowej. WAT, Warszawa
- [15] Budzik G. (2007). Synteza i analiza metod projektowania i wytwarzania prototypów elementów o skomplikowanych kształtach na przykładzie wirników turbosprężarek. Oficyna Wydawnicza Politechniki Rzeszowskiej, Rzeszów
- [16] Nowicki M. (1978). Lasery w technologii elektronicznej i obróbce materiałów. WNT, Warszawa
- [17] Laser Technik Journal (2012) Vol. 4, WILEY-VCH Verlag GmbH&Co. KGaA, Weinheim, pp.28-33
- [18] Darlewski J. (1978). Obróbka skrawaniem tworzyw sztucznych warstwowych. WNT, Warszawa
- [19] Zalecenia obróbki półwyrobów z tworzyw sztucznych. (in Polish) <http://docplayer.pl/14155883-Zalecenia-obrobki-polwyrobow-z-tworzyw-sztucznych.html> (4.05.2018)
- [20] Klimpel A. (2012). Theoretical basis of laser cutting of metals, Przegląd Spawalnictwa 6, pp. 2-7,
- [21] Šuba O., and others (2018). Modelling of a transient-temperature field in plastics during laser cutting, Materials and Technology, 52,1 pp. 19-21
- [22] Zaborski S., Stechnij T. (2011). Laserowe i plazmowe cięcie blach ze stali niestopowych i kwasoodpornych, Inżynieria Maszyn, 16/4, pp. 109-116

- [23] Skoczylas A. (2012). Analiza porównawcza procesu cięcia wiązką laserową i strumieniem wodno-ściernym, *Postępy Nauki i Techniki*, 8, pp. 121-128
- [24] Trzepieciński T. (2012). Trendy rozwojowe maszyn i technik stosowanych w [technologiach cięcia blach, *Inżynieria Maszyn*, 17/3, pp. 94-106
- [25] Some words about machining of plastics, (2018)  
CADblog.pl, 3(04) May 2009, pp.37-38,  
[https://www.cadblog.pl/archiwum/CADblogpl\\_nr\\_3\(4\)\\_2009\\_LQ\\_v2.pdf](https://www.cadblog.pl/archiwum/CADblogpl_nr_3(4)_2009_LQ_v2.pdf)
- [26] Powel J. (1998). *CO<sub>2</sub> Laser Cutting*, Springer-Verlag London Limited, pp.91-100,
- [27] Banasiak A. and others, Właściwości kompozytów polimerowych PE+TALK, *Kompozyty 2* (2002), pp. 126-130
- [28] Pikosz P. and others (2016). Wpływ zawartości talku w LDPE na właściwości kompozytu, *Tworzywa sztuczne w przemyśle* No 3, pp.52-58

## Chapter 2.

Olha DVIRNA<sup>1\*</sup>

# INFLUENCE OF THE CUTTING TOOL PROPERTIES ON THE TREATMENT SURFACE QUALITY IN THE HEAT RESISTANT STEEL BROACHING

### Abstract

The article presents the results of research on the influence of surface quality and geometry of broach teeth made of two types of high-speed steel on the roughness of samples made of heat resistant steel. A comparative analysis of two broaches tools with different geometry and sharpening method was performed, as well as a method of deburring taking into account the high quality of the broach teeth surface. As a result of tests, it was found that broaches made of high-speed steel SW7M guarantee the highest quality of the machined surface of the lock grooves of gas turbine discs. The clearance angle value should be  $\alpha = 3^\circ \pm 15'$  in the absence of a chamfer on the clearance surface with angle  $\alpha = 0^\circ$ . Finishing the broach teeth using a cubonite wheel with KM40/28BG150% characteristics ensures roughness Ra 0.036-0.06  $\mu\text{m}$  and guarantees no overheating of the tool at peripheral speeds not exceeding 25 m/s. The best results in the deburring of the rake broach teeth surface were obtained with abrasive tools type 54C 10P GM B5 (the roughness of the surface of the lock groove treated with this tool is Ra 0.7 ... 0.9  $\mu\text{m}$ ). The use of diamond tools ensures deburring but leaves flaws at the edges in the form of unevenness. The mechanism of micro unevenness of machined surfaces in the broaching process is determined by the cutting profile and its roughness. Due to the above, it is necessary to research and analyze of the edge and the surface quality of the broach teeth, ways of sharpening and finishing them with the appropriate shape and geometry of the cutting edge, selection of appropriate grades of tool steel and fluids or lubricants improving machinability new types of heat resistant steels.

**Keywords:** shape accuracy, surface layer quality, lock grooves broaching, heat resistant steel, sharpening and finishing.

---

<sup>1</sup>Faculty of Marine Engineering, Gdynia Maritime University, 81-87 Morska Str. 81-225 Gdynia, Poland

\*e-mail: o.dvirna@wm.umg.edu.pl

## 1. Introduction

Increase of the new gas turbines capacity, accompanied by an increase in operating temperatures, stresses, vibrations, etc. It leads to a steady increase in requirements for materials used for their manufacture [2]. New grades of heat resistant materials need to be developed and introduced [3]. The introduction of such materials is complicated by the lack of research in the field of their treatment by broaching [4]. During cutting by traditional technology, the quality of the surface does not meet design requirements, many defects are formed in the form of burrs, ripples, rolling-and peening, etc., which is unacceptable in terms of complex intense operation conditions of the interlocks. That may result in reduced reliability of the attachment, damage of the tail part of the blades, disk rim and engine as a whole [1]. That is why the researches, which to ensure the major parameters of the surface layer quality of the turbine and compressor disks grooves made of ЭП517 III steel are necessary. The mechanism of treatment surface quality formation in the broaching is determined by the forming part of the cutting edge and its micro roughness. Therefore, it is necessary to give one's attention to the broach's teeth quality, their sharpening, and finishing.

## 2. Study the material and the method of sharpening broaches

Broaching tools for cutting heat-resistant materials are usually made of different grades of high-speed steels. For experimental the cutting tool material grades were selected: P18, P6M5 (toughness – 40...65 N/cm<sup>2</sup>) and P6M5K5MII (toughness – 15...20 N/cm<sup>2</sup>). These tools broached three grooves in the turbine disk was made of heat-resistant steel ЭП517 III. Then broaches were sharpened and the experiment was repeated. The cutting edge surface was monitored after each experiment under a microscope with a magnification of 56 times. As a result on the surface cutting edges of the broach made of steel P6M5K5MP numerous defects were defined but on the cutting edges of the broaches made of steel P6M5 are single and minor. That's why the high-speed steel P6M5 was chosen to use for ensuring the best treatment surface quality.

To study the effect of design features and the method of sharpening broaches on the surface roughness of the treated surface, two broaches made of steel P6M5 were selected (fig. 2.1).

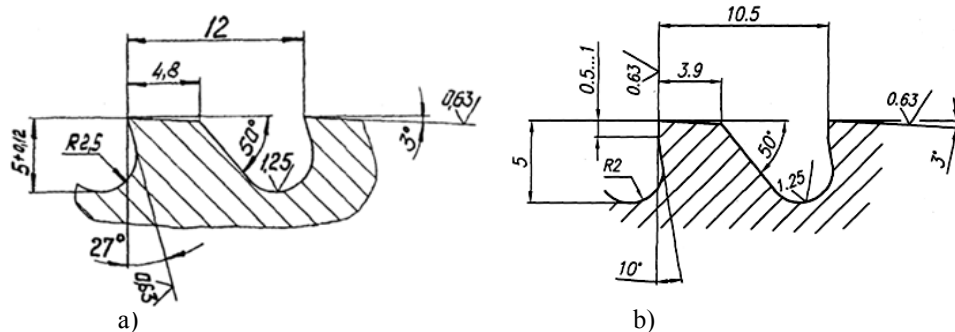


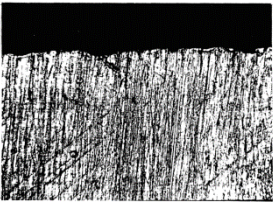
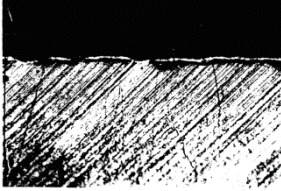
Fig. 2.1 Broach's teeth geometric parameters a) type A; b) type B

The first one (type A) broached 12 turbine discs without resharpening with satisfactory grooves surface quality. The second one (type B) did not ensure the necessary level of roughness grooves surface on any of the discs. To find out the reasons for that a comparative analysis of the broach's teeth quality was performed (realized). The results of the analysis are shown in table 2.1.

Table 2.1. The comparative analysis of the broach's teeth quality

Investigated parameter	Broach's teeth	
	Type A	Type B
1	2	3
The broach's teeth hardness	HRC 65	
Material structure	a) grain sizes - №10...11 of the scale (GOST5639-82); b) the microstructure is satisfactory - martensite and carbide; c) carbide heterogeneity – 2 <sup>th</sup> level of the scale (GOST19265-73)	a) grain sizes - №9...10 of the scale (GOST5639-82) b) the microstructure is satisfactory - martensite and carbide; c) carbide heterogeneity – 2 <sup>th</sup> level of the scale (GOST19265-73)

Continuous of table 2.1.

1	2	3
The roughness of the broach's teeth flank face (the value designated in the drawing is Ra 0,32 μm)	Ra 0,22...0,44 μm	Ra 0,27...0,46 μm
The calibrating broach's teeth orthogonal clearance angle (the value designated in the drawing is $\alpha = 3^\circ \pm 15'$ )	$\alpha = 3^\circ$	$\alpha = 0^\circ$
The cutting edges condition of the calibrating broach's teeth (the character of surface microrelief)	<p>a) the traces of sharpening are removed;                      b) the direction of the traces are parallel to the broach axis, that facilitates chip flow during processing</p> 	<p>a) there are traces of sharpening;                      b) the direction of the traces is at an angle to the broach axis, which makes it difficult to remove the chips during processing</p> 

From the comparative analysis presented in the table 2.1, it follows that the material quality and heat treatment of both broaches are satisfactory. Low wear resistance and unsatisfactory surface quality of broached grooves in the disc are not related to material quality and heat treatment of type B broach. The surface defects are mentioned above are caused by poor chip removal from the cutting zone. As a result, the temperature in this area increases and the processes of hardening and adhesion are intensified. The surface quality of the broached grooves in the disk is reduced (numerous defects on the surface processed and high level of the roughness). Therefore, for finishing broaching is recommended to increase the teeth pitch so that the cutting process is carried out by a single tooth. The teeth pitch of the broaching tool should be no less than the length of the groove in the disk. Such a construction solution the traces were formed on the surface broached groove is eliminated.

The cutting edges surface both of the type broaches were also researched on a “Camebax” micro analyser. On the cutting edges of the broach type B, the ubiquitous metal adhesion was observed. As a result of the adhesion, the cutting edge was thickened for along the whole its length. By the X-ray analysis method was identified the adhesion and the base material of the type B broach. It shows that the adhesion metal was formed on the cutting edges during the sharpening process.

To improve sharpening and finishing quality of broaches cutting edges the grinding wheel on the organic bonds with graphite filler was tested. That was produced by Scientific Production Enterprise “Precision Abrasives” (Ukraine).

Grinding wheel types:

1. 12A2-45° 75×3×3×16 KM 40/28 БГ 150% - 2 pieces;
2. 12A2-45° 75×3×3×16 KM 20/14 БГ 150% - 2 pieces;
3. 12R4 75×3×2×16 KM 40/28 БГ 150% - 2 pieces;
4. 12R4 75×3×2×16 KM 20/14 БГ 150% - 2 pieces.

Broach material - steel R6M5. Before finishing, all the broach's teeth were sharpened by grinding wheel made from electro corundum and numbered by an electric spark method. Finishing of the rake and flank faces of the broach teeth on was carried out on machines B3-495Φ1 and 360M. Finishing with a cubonite grinding wheel with a KM 20/14 BG 150% characteristic is showed that the cubonite grinding wheel provide a roughness of  $R_a = 0.036 - 0.06 \mu\text{m}$ . But it's do not guarantee the absence of grinding burn, especially on machine tools with manual control. Therefore, further work on broaches teeth finishing was carried out with KM 40/28 BG150% cubonite grinding wheel.

After finishing, the teeth were cut from the broach by an electric spark method. To measure the rake face roughness on the body of the teeth, a horizontal platform was ground, lying in the same plane as the teeth rake face. The sharpening stone “Arkansas” was manually removed the smallest burrs formed in the finishing of the rake and flange face broach teeth. The teeth prepared in this way were measured on the cutting edge straightness. Then the roughness of the rake and flank faces was measured with the Surface Roughness Testers (Electronic Profilometer model 296) and the rake surface was photographed with the “Neophot” microscope (zoom of 100 times). The results of measurements of the rake and flank face roughness have been shown in table 2.2.

Table 2.2. The rake and flank faces roughness of the broach teeth

The cutting tooth number	Condition of machining			Roughness Ra, $\mu\text{m}$		Grinding burn
	Speed	Feed		the flank face	the rake face	
	V, m/s	S <sub>t</sub> , mm	S <sub>s</sub> , mm/min			
1	25	0,005	500	0,08...0,09	0,20...0,32	
2	20			0,08...0,10	0,22...0,35	
3	15			0,06...0,10	0,20...0,32	
4	25		1000	0,07...0,09	0,25...0,35	
5	20			0,08...0,09	0,32...0,40	
6	15			0,07...0,09	0,35...0,40	
7	18	Manual		0,07...0,08	0,25...0,30	
8	36		0,05...0,07	0,20...0,35	burn	
9	28		0,05...0,06	0,25...0,32	burn	
10	14		0,07...0,09	0,15...0,18		

As can be seen from table 2.2, when finishing with peripheral speeds of 28 m/s and 36 m/s, the grinding burns appeared on the treated surfaces of the broach teeth, therefore the peripheral speeds should not exceed 25 m/s. Deviations from straightness of the cutting edges on all teeth did not exceed 0.005 mm. However, in the photo single defects were found on the cutting edges in the form of an irregularity stretched along the edge with a length of 1 ... 1.5 mm and a depth of 0.01 ... 0.02 mm. These defects could have been formed by manually removing the burrs on the cutting edges with the sharpening stone "Arkansas". This assumption was confirmed by measurements of the roughness of the back surface of the teeth and the radius of rounding of the cutting edge before and after removal of the burr. These measurements are shown in table 2.3 and 2.4.

Table 2.3. The roughness of the flank face teeth before and after removal of the burr Ra,  $\mu\text{m}$

	The number of the investigated tooth									
Before	0,075	0,067	0,071	0,073	0,076	0,068	0,051	0,044	0,038	0,061
After	0,085	0,090	0,085	0,080	0,085	0,080	0,075	0,060	0,055	0,080

Table 2.4. The radius of the cutting edge before and after removal of the burr,  $\mu\text{m}$

	The number of the investigated tooth									
Before	5-5,5	2,5-5,5	6,5-7	3-4,5	-	-	-	-	-	-
After	7,5-8	9-10	edge defect	6-6,5	4-5	10-15	4-5	3-4	6-7	5-8



In order to ensure the stability of the broached surface quality in the grooves gas turbine discs made of steel EII517-III various methods of removing the burrs on the cutting edges were studied. For the experiment, was prepared samples of the brooches teeth so that it allowed to photograph the cutting edges on the “Neophot” microscope. The broaching teeth material is high-speed steel P6M5 (HRC 65 ... 67). The tooth samples were finished by following technology: the front rake face was finishing with cubonite 12R4 75×3×2×20 KP 50/40 B1-13 150%; the flank face with 12A2-45° 75×3×3×20 KP50/40 B1-13150%. However, such technology leads to the burr formation on the rake face of the cutting edge. For the elimination of these burrs, different methods of finishing were used. Then the teeth surfaces roughness was measured on the model 296 profilometer, and on the metallographic microscope were made rake face photographs of the cutting edges. The results of the roughness measuring of the rake and flank faces, before and after burrs removal, are shown in table 2.5.

Table 2.5. The roughness of the broach teeth surface

Number of the broach teeth	The surface roughness Ra, μm			
	before burrs removal		after burrs removal	
	rake face	flank face	rake face	flank face
1	0,24...0,30	0,22...0,24	0,25...0,30	0,24...0,25
2	0,25...0,32	0,28...0,30	0,25...0,32	0,27...0,30
3	0,17...0,26	0,28...0,32	0,17...0,26	0,29...0,32
4	0,16	0,25...0,32	0,16	0,27...0,32
5	0,26	0,24...0,27	0,25...0,27	0,23...0,28
6	0,28...0,32	0,28...0,32	0,28...0,32	0,30...0,32
7	---	---	0,20...0,24	0,25
8	---	---	0,23	0,20...0,27

The best result was obtained when using the sharpening stone of type 54C 10II GM B5 . The use of the diamond stone, although it provided for the burr removal, but left defects on the cutting edge. The organic material did not remove the burr (fig. 2.2).

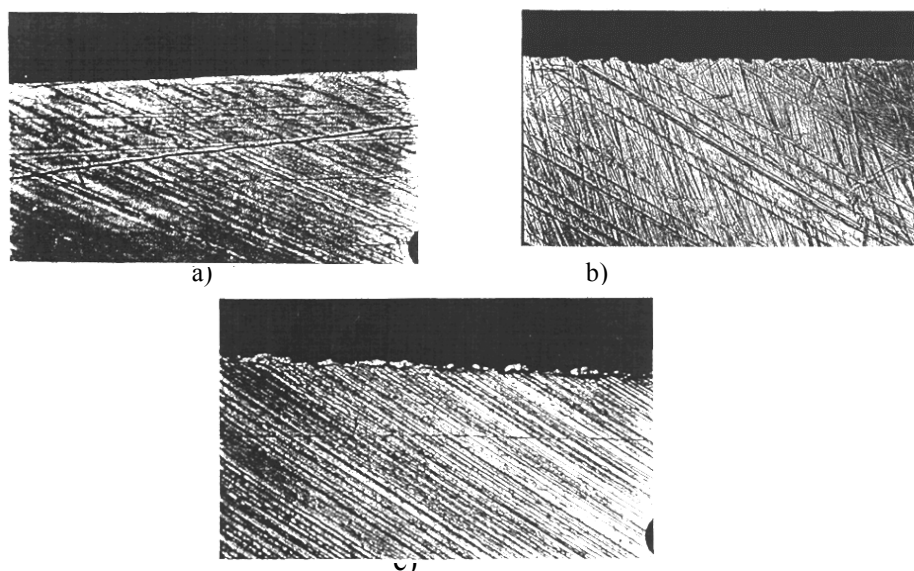


Fig. 2.2 . The photos of the cutting edges after the deburring by different sharpening tools

Explanations for fig. 2.2 are shown in the table 2.6.

Table 2.6. The cutting edges condition after deburring

Designation on fig. 2.2	Finishing tool	Cutting edge condition
a)	Sharpening stone 54C 10П ГМ B5	Removed burr and micro roughness on the cutting edge
b)	Diamond stone ACM 40/28 P33 50%	Removed burr but micro roughness on the cutting edge height of 4 ... 10 microns is observed
c)	Organic material	The burr did not remove

After sharpening the cutting edges of broach teeth by various methods the locking grooves were broaching in the turbine disc made of  $\text{ЭП517-III}$  steel. In tab. 2.7 have been shown the results of measuring the surface roughness of these grooves.

Table 2.7. The dependence of the finishing tools and the surface roughness

Type of finishing tool	The surface roughness of the locking grooves Ra, $\mu\text{m}$
Sharpening stone 54C 10П ГМ B5	0,7...0,9
Diamond stone ACM 40/28 P33 50%	0,9...1,2

As can be seen from table 2.7, the treated surfaces roughness is less when using an sharpening stone. As a result of the conducted research, the methods of sharpening and finishing the cutting edges of broach teeth were defined. These methods have been ensured the highest surface quality of the grooves were being broached.

### 3. Study of liquids for broaching

For heat-resistant steels cutting at the machine enterprises of Ukraine, liquids are used, such as: “Sulfofresol”, Ukrinol-5/5 (-14, -202); OSM-1 (-3), etc., but the most effective in terms of technological and sanitary-hygienic parameters are liquids of the type “Asfol”, “Nikvol”. Physical and chemical parameters of these liquids are given in tables 2.8 and 2.9.

Table 2.8. Physical and chemical parameters of liquid “Asfol”

Parameters	Values for liquid type	
	“Asfol –	“Asfol -2”
Appearance	The liquid is oily from brown to dark brown color	
Smell	With a characteristic smell of olive	
Density at $(20\pm 1)^\circ\text{C}$ , $\text{g}/\text{cm}^3$	0,850 – 0,960	0,880 – 0,990
Relative viscosity * - by VZ-246 viscometer with a nozzle diameter of 4 mm, at $(20 \pm 1)^\circ\text{C}$	18 – 90	24 – 124
Pour point, $^\circ\text{C}$ , not less	-2	-2
Metals Corrosion Tests: - steel - aluminum - copper	withstand withstand withstand	withstand withstand withstand
Mass fraction of mechanical impurities,%, not more than	0,5	0,5
Flash-point in an open crucible, $^\circ\text{C}$ , not less	140	140

Table 2.9. Physical and chemical parameters of liquid “Nikvol”

Parameters	Values for liquid type	
	“Nikvol - RO”	“Nikvol - MM”
Appearance	The liquid is oily from brown to dark brown color	
Smell	With a characteristic smell of olive	
Density at (20±1)°C, g/cm <sup>3</sup>	0,850 – 0,960	0,880 – 0,990
Relative viscosity * - by VZ-246 viscometer with a nozzle diameter of 4 mm, at (20 ± 1) ° C	18	24
Pour point, ° C, not less	- 2	- 2
Metals Corrosion Tests: - steel - aluminum - copper	withstand withstand withstand	withstand withstand withstand
Mass fraction of mechanical impurities,%, not more than	0,5	0,5
Flash-point in an open crucible, ° C, not less	195	195
Kinematic viscosity at (50 ± 1) ° C, mm <sup>2</sup> /s, not less	10	15
Liquid stability during storage	withstand	withstand

These liquids are universal and are used for various types of "heavy" processing.

Their use is most appropriate due to extreme lubricating and deburring properties. So, “Asfol” and “Nikvol” liquids can be used for broaching lock grooves of the turbine and compressor disks. To select the most suitable liquid the experiment was carried out on planning and broaching machines in a wide cutting speed range from 1 to 28 m/min.

For broaching the lock grooves in samples made of EP517-Sh steel at the speed of 1 m/min the “Nikvol” liquid was used. That reduced process of chips sticking on the cutting edge of the broaching teeth compared with dry broaching and with other types of liquids. The defects on the groove surface weren't observed. The surface roughness was at the level of the design requirements for this element (Ra 0,63 ... 1,25 microns). During the "dry" broaching, ubiquitous metal covering, gaps and ripples were observed. The surface roughness exceeded Ra 3,5 microns (see fig. 2.3, 2.4).

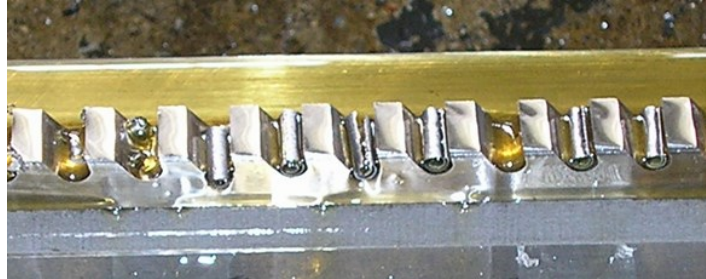


Fig. 2.3. Broaching cutting element with formed chips



a)



b)

Fig. 2.4. The groove surface after broached: a) with using liquid, b) "dry" cutting

The use of "Nikvol" liquid reduces the tendency of heat-resistant materials to the processes of adhesion under conditions of high contact stresses at low cutting speeds. During the "dry" broaching the wear process of the cutting edge is intensified and the surface quality is deteriorated. In fig. 2.5 is shown broach teeth wear during the "dry" cutting.



Fig. 2.5. Broach teeth wear during the "dry" cutting.

#### 4. Conclusions

As a result of the research, recommendations were developed and implemented to ensure the major parameters of the surface layer quality of the turbine and compressor disks grooves made of EP517-Sh steel by improving the technology of their broaching:

- use of finishing broaches made of P6M5 (P18) steel;
- the clearance angle value of the broach's finishing teeth is  $\alpha = 3^\circ$ ;
- the flank face roughness of the teeth should not exceed  $Ra = 0,32 \mu\text{m}$ ;
- sharpening of the flank and rake faces of the broach's teeth must be performed with KM40 / 28BG150% cubonite wheel at the speed of  $V = 15 \dots 25 \text{ m/s}$ ;
- removal of the burr from the flank face of the broach's teeth should be performed with an 54C10ПГМБ5 sharpening stone;
- use of "Nikvol" liquid to ensure the surface quality of the lock grooves and reduce the wear of the broaching tools during finishing operations.

#### References

- [1] Bogatov, A. A., Mechanical properties and models of metal destruction, Ekaterinburg 2002.
- [2] Boguslaev, V. A., Muravchenko, F. M., Zhemanyuk, P. D., Kolesnikov, V. I., et. al., Technological support of operational characteristics of GTE parts. Compressors and Turbines. Part I Monograph, 'Motor Sich' JSC, Zaporozhye 2003.
- [3] Dvirnaya, O. Z., Shumilov, A. P., Research of the quality of the machined groove surface in samples of steel EP517-III, Actual problems of mechanical engineering: Materials of the International Conference, NUK, pp. 137-138, Mykolaiv 2011.
- [4] Dvirnaya, O. Z., Shumilov, A. P., Modern methods of processing the locking grooves in the GTE, Actual problems of engineering: Materials of the International Conference, NUK, pp. 112-115, Mykolaiv 2011.

## Chapter 3.

Józef BRZĘCZEK<sup>1</sup>

# POSSIBILITIES OF IMPROVE THE PRODUCTIVITY OF OPERATIVE PROGRAMS

### Abstract

The basic problem of the preparation and implementation of piece and small lot production is the cyclical preparation of variable production programs and the need to modify them during the execution. The causes of current corrections are random events: failures, cancellation of orders, special orders and lack of load or overload of production resources. Productivity is one of the company's competitiveness parameters, defined by the level of utilization of the resources available. Productivity can be presented as the maximization of the effects (level of achievement of goals) with the available resources as well. The minimization of the resources used, emphasized in the optimization issues, is inadequate because the company have are constant values independent of the size of the production programs. The enterprise has a limited influence on the size of orders, therefore, the improvement of productivity can only be carried by increasing the level of utilization of the available production resources. Often, the assessing of the productivity of a company is presented by profitability thresholds, are taken as measures. The paper analyzes the traditional methods of improving productivity in relation to the type of production under discussion and proposes the use of discrete optimization as a tool for managing production processes. Practical solutions for improving productivity through corrections were presented adjustments in optimized operational programs and the legitimacy of their application.

### Keywords:

productivity, piece and small lot production, labor-consuming, scheduling, learning and forgetting curves, optimization.

---

## 1. Introduction

Production programs of mixed piece and low-series production are the most complex organizational issue of preparation and implementation of production

---

<sup>1</sup>Faculty of Mechanics and Technology, Rzeszow University of Technology,  
Kwiatkowskiego 4, 37-450 Stalowa Wola, Poland. e-mail: j.brzeczek@prz.edu.pl

processes. The basic problem of this type of production are cyclical changes of its (usually set in monthly intervals) and their modification during execution. The reasons for the modification are events, eg failures, withdrawal of orders or special orders, which requires ongoing changes and corrections. The measure of productivity<sup>3</sup> is also a parameter of the competitiveness defined by the level of use of available enterprise resources. The term resources means: human resources (here understood as the available work capacity of work stands), capital resources including work stands, devices, infrastructure, materials, energy, technologies, everything that can be used in the production or services. The productivity of enterprises can be considered as partial, productivity of capital, total productivity and so on. The maximization of the utilization of the available resources to  $U_i$  of the company executing the operational program (15,16) can be expressed in various measures: natural, cost of used resources in %, the form of minimizing unit fixed cost by maximizing the use of available resources. In practice, the profitability approach in the so called short settlement period is focused on maximizing profit, which is not tantamount the increase productivity [5]. For analysis of operational programs, the following criteria are distinguished: cost (additive type of value) and resources (usually additive type). In the article, the analysis of the resource criterion understood as the total amount of used time resources (labor-consuming) of available work stands was adopted as the basis of productivity analysis. With this assumption, productivity is understood as maximizing the size of production with the available time resources. Regardless of the analyzed area of the company's operation, certain measurable parameters must be adopted, as well as units and a reference system to present and compare the production results. The minimization of used resources for realized operational goals, emphasized in the optimization issues, is an inadequate criterion, because they constitute a constant quantity independent of the size of production programs. Productivity improvement can be achieved by increasing of available resources consumption. The enterprise productivity assessment proposed in the article makes use of profitability formulas, and the expression of the level of utilization of the available resources and their reference to the size of production has been presented in natural measures. The paper discusses the practical possibilities of improving the use of resources and the legitimacy of their use.

## **2. Assessment of productivity of operational programs**

The company has a limited impact on the price of the products and services offered, the size of orders for goods and services and other external factors, hence the focus has been on improving the use of resources (internal factors), which in

---

<sup>3</sup>There are many definitions of productivity, in economic terms it is "the size of the production effect obtained from the given inputs"



the financial measure is expressed by the desire to minimize costs. The analyzes carried out concern the so-called short periods, i.e. without changes in the technologies available, investment activities and assuming no rotation of the crew. Soft productivity improvement tools such as: the global approach model MFPMM, KAIZEN, 5S, Pareto-Lorenzo charts, etc., and awareness of the crew in this area, are important, while the article attempts to analyze the use of the so-called. hard tools in the form of mathematic formulas and software that gives quantitative information on the possible level of productivity improvement of operational programs. As a basis for the analyzes, the use of available working time at workstations was adopted with the support of the financial measure of the costs of indirect labor and intermediate materials added by the accepted settlement key [6]. The labor consumption of direct labor includes the specificity of workstations, eg one employee on several positions or several employees on one workstation. This approach allows the assessment of productivity by operating the workload of orders and the available resources of working time. The total costs of the operational programs implemented in the settlement period in question can be described by formulas (1,2):

$$K_C = K_Z + K_S = \sum_{p=1}^R P_p \sum_{i=1}^n k_{zi} x_i + \sum_{l=1}^k S_l \quad (1)$$

where:

$K_C$  - total cost of the completed production program;

$K_Z$  - total variable cost of the production program;

$k_{zi}$  - unitary variable cost of the  $i$ -th product (the formula is right assuming that the variable cost is not a function of the production size) referred to the work stands;

$S_l$  - unit (separated) fixed costs in the departmental and general in the settlement period, added from the system, eg. to the cost of *rbg* .

$i$  - order, production batch, tasks;

$l$  - number of separated fixed costs components ( $l = 1, 2, \dots k$ );

$P_p$  - number of orders (tasks).

$$S_l = \sum_{j=1}^m \sum_{i=1}^n a_{ij} x_i (1 - h_j) \quad (2)$$

where:

$a_{ij}$  - unit share of  $j$  - of this resource (*Rbg*) incurred for the implementation of  $i$  - this product. In practice, this is a function of the production quantity(6,7);

$h_j$  - unit indirect cost added with the summation  $a_{ij}$ .

$h_j$  - amount of resources understood as fixed costs  $j$  assigned to the performance of the  $i$ -th product, e.g. in *Rbg*;

- $n$  - the number of items / orders in the operational program including work-in-progress;
- $m$  - the amount of resources (fixed costs) and added to the production realized under the analyzed production program (*rbg*);
- $x_i$  - the amount of production  $i$  - in natural or contractual units<sup>4</sup>.

The relation  $K_s$  expressed productivity in a financial measure related to the total realized production of individual products in accordance with formula (3):

$$P_{rw} = \frac{\sum_{i=1}^n n_i c_i}{K_s - \frac{\sum_{i=1}^n n_i k_{zi}}{\sum_{i=1}^n n_i c_i}} \quad (3)$$

where:

- $\sum_{i=1}^n n_i c_i$  - production value expressed in sale prices;
- $K_s$  - total fixed costs of the economic unit in the settlement period;
- $\sum_{i=1}^n n_i k_{zi}$  - the sum of unit-variable costs in the settlement period;
- $n_i$  - the quantity of manufactured  $i$  - th products including production in work;
- $k_{zi}$  - variable cost of the  $i$ -th product at the production volume under consideration;
- $i$  - another product assortment of production.

### 2.1. Technical and organizational preparation

The criterion of productivity assessment may be expressed as the total unit cost of labor of a contractual or natural product, or the number of used *Rbg*. Maximizing of productivity will be the minimize these costs, which will be reduced by maximizing the use of available resources. Optimizing productivity means minimizing the unit labor-consuming by maximizing the rationally justified use them related to the product or service. The resources are included in fixed costs, can by the improvement as unitary terms achieved by their total reduction or maximization of their use<sup>5</sup>. The issue is difficult to analyze, because

<sup>4</sup>The use of contract units allows us to model the share of non-finished production and finished products that will always appear in production processes.

<sup>5</sup> It was assumed that the company does not have fixed unjustified costs (pays) due to incorrect organization or unsuccessful investments, eg unprofessional working positions

of organization of enterprise<sup>6</sup>, available resources and the competencies of individual employees. Resources treated as fixed costs are: administration (trade, supply) and management as well as employees from technical and quality divisions, production and auxiliary facilities. The administration and the technical departments of the unit and low-volume production enterprises, will be relatively bigger and will require the employ the better experienced workers. These people must be the person who can work and undertake technical current decisions. The analysis of this area of the enterprise, is the subject of the study and estimation of the level of productivity. The essence of results this area of activity are ensue from the necessity of cyclical technical and organizational preparation as well as ongoing corrections of operational programs for the following reasons:

- a. production programs are prepared (technical and organization) cyclically, and the share of repetitive production is small quantity;
- b. for each order it is required to prepare at least a simplified technological processes at the level enabling settlement of scheduling and materials;
- c. the occurrence of organizational disorders due to special orders and / or changes in the dates of their implementation [5];
- d. random events regarding ordered parts and the execution<sup>7</sup>.

The labor consumption and materials use for the mentioned type of production are determine on base of technological standards specific to the enterprise and the available work stands. The organization of production processes is characterized by the following parameters:

- a given number of production orders is considered in each accounting period. The company operates on a continuous basis, therefore in operational programs there are uncompleted orders, which go to the next accounting periods at the level of the current implementation and are treated as full in each new settlement period;
- for each order, a basic technology is prepared at least level to determine the required labor-time, resources (broken down into workstations planned for use) and direct material resources;
- resources and intermediate materials are added from the prepared formulas, eg to labor time;
- technological processes of each order clearly define the success of technological operations that can't be changed;

---

or unnecessary administrative services. It was further assumed that owned resources are reasonably used in executed orders.

<sup>6</sup> Formal and legal requirements as health and safety requirements, qualitative and specific industry requirements.

<sup>7</sup> To simplify the issue, it was assumed that there are no problems with material deliveries.

- individual operations can't be interrupted;
- each work stands can perform only one technological operation and each operation can be performed only at one workstation (in practice, such a limitation may not occur);
- orders can be divided into production batches. After dividing, production parties are treated as separate orders;
- individual orders may have additionally imposed deadlines for the start and completion of individual orders;
- the available resources can be temporarily increased by working overtime, including by launching the second or third shift.

The preliminary assessment of the use of the production resources of the company (with an estimated analysis of the combination of the program with resources) is made by balancing the available resources with the required resources [6]. The balancing of working time resources is represented by formulas (4, 5):

$$\mathfrak{J}_w = \sum_{j=1}^m J_j \quad (4)$$

where:

- $\mathfrak{J}_w$  - labor consumption of the operational program;
- $J_j$  - labor consumption of orders;
- $m$  - the number of orders in the operational program.

The necessary labor time for completing the production lot (order) with given simplifying assumptions is presented in (5):

$$J_j = \sum_{j=1}^m \left( \frac{t^{n_{pzj}}}{n} + \left( \sum_{n=1}^s (t^{n_{gj}} + t^{n_{pj}})(1 + k_{uj}) \right) \right) \quad (5)$$

where the components (specific for the plant and production departments) mean:

- $s$  - the number of pieces of the product in the production batch;
- $j$  - number of technological operations;
- $t^{n_{pzj}}$  - preparation and completion time, depending on ( $n$ );
- $t^{n_{gj}} = f(n)$  - main time;
- $t^{n_{pj}} = f(n)$  - auxiliary time;
- $k_{uj}$  - technological coefficient.

Required resources include the times of planned repairs, but random situations haven't been taken into account. In the case of special events, the use of overtime work or the negotiation of termination dates is accepted. Activities aimed at

improving the use of resources may be conducted in the following areas: technical, technological and organizational.

### **3. Technical and technological possibilities to improve productivity**

Preparation of operative programs for the majority of orders should be considered as the processes of starting a new production, so the starting factors are used. For orders that are similar from technological point of view, the preparation of production documentation are based on the analysis of technological feasibility, valuation (normalization) of labor consumption and material requirements. The materials (direct and indirect) are valued based on the norms. The costs (resources) of the company's quality services are accounted for as fixed costs. The problems are complicated when accepting orders are significantly deviate from the standard technological processes. In such cases, the issue from the launch of new production should be analyzed [3]. Such orders should be excluded from the productivity analysis, because it's really different and should be considered in the nature of the investment for example of adapting work stands or implementing new technology. In the presented analysis it was assumed that the orders don't require any special and additional activities, and the additional requirements are taken into account with corrections  $t_{pz}$ . In the low serial production carried out irregularly there is a limited possibility of achieving normal production efficiency, and interruptions in the implementation of specific calls may cause the effects of forgetting production habits. With larger orders, longer breaks and a relatively high percentage of manual operations, the effects of these phenomena may be significant [5] and should be included in the planned consumption of resources.

#### **3.1. Experience curve**

The experiment curve (the curve of habits, the phenomenon of productive learning) is observed with the increasing number of performing the same manual activities, without interruptions in their performances [4]. The effect of such implementation is a decrease in the unit labor time  $t_n$  of the next items in the lot, in a quantitative increase of production and usually a decrease in the number of non-conforming products<sup>8</sup>. For production carried out in the form of job-shop production, the formula T.P. Wright's is assumed as the empirically confirmed formula describing this phenomenon of production learning (6):

$$t_n = t_1 n^{-\alpha} \quad (6)$$

---

<sup>8</sup> There is also a degradation of the unit cost -  $kz_j$ , but slower than unit labor consumption  $t_n$ , which results from the fact that labor consumption is one of the components of the variable cost. Charts describing the phenomenon selected for analysis require adjustments related to the specificity of the business entity and the participation of manual operations.

where:

- $t_n$  - unit labor consumption of  $n$  -th of this product;
- $t_1$  - unit labor consumption for the first product;
- $\alpha$  - empirical degradation coefficient of unit labor consumption;
- $n$  - number of the next product.

Generalized phenomenon of acquiring experience expressed in reducing the time of performing a technological operation for simple manual operations is shown in Fig. 3.1. The result is a shortening of the time needed for the implementation of specific technological operations, and thus an improvement in the use of the work station.

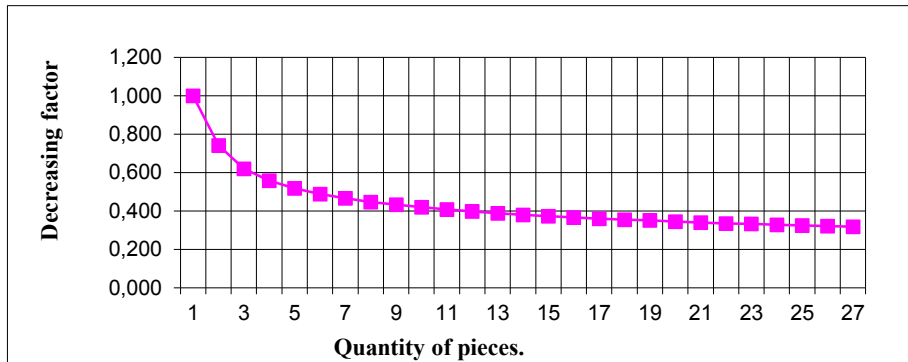


Fig. 3.1. An example of an experimental curve run for simple manual operations. *Source: own study.*

### 3.2. The curve of forgetting

Breaks in the execution of orders of the same products cause the occurrence of the phenomenon of forgetting production habits which is dependent on the size of the time intervals between subsequent starts, sizes of particular batches, preparation and experience of employees, preparing of work-stands and the participation of manual operations. The phenomenon of forgetting skills and production habits, also known as the curve of disappearance of practice, has a course similar to the curve of forgetting described by H. Ebbinghaus. The quantitative determination of the effects of the omission of habits [4] requires the collection of empirical data, specific for a particular technology and department, and can be expressed by the increase in the technological time of operations, and thus the deterioration of productivity (7).

$$\omega = \frac{100V}{(\log t)^\varepsilon + V} \quad (7)$$

where:

- $\omega$  - the inverse of the duration of the operation;
- $\varepsilon, V$  - experimental constants;
- $t$  - time from the moment of discontinuation of a specific technological operation.

An example of the course of the curve of forgetting production habits for simple manual operations in the form of a relative increase of unit work time is shown in Fig. 3. 2. With the implemented technologies, good stands equipment and a relatively small proportion of manual operations, the decrease in labor intensity due to acquiring and forgetting skills can be slight. Changes in the consumption of resources due to the phenomenon of learning and forgetfulness in the conditions of the discussed type of production are taken into account by using coefficients depending on the number of pieces in the production batch, and in the case of new implementations of the so-called start-up coefficients. Mentioned coefficients don't take into account the length of breaks between the similar orders. Decisions regarding the qualification of such orders are treated discretionally in accordance with the assessment of the implementation of technology. In the case of implementing new technology or complex new products, it is advisable to conduct the commissioning analysis [3] or analysis using, for example, network methods and taking into account the risks at individual stages of implementation.

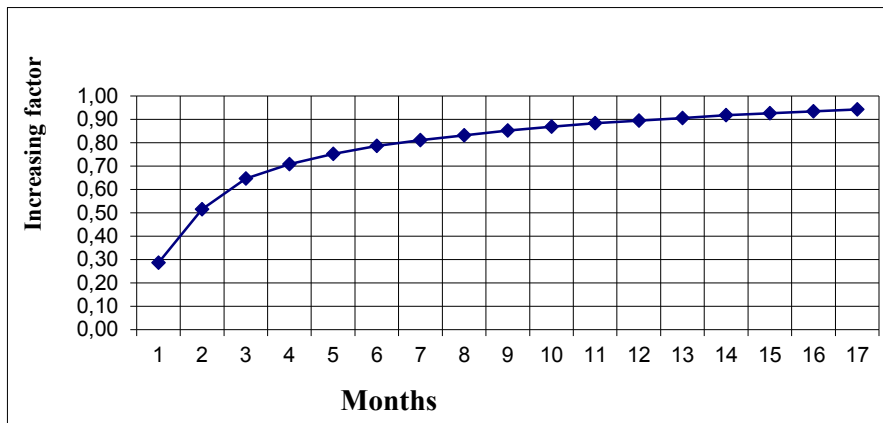


Fig. 3. 2. An example of a forgetful curve for simple manual operations.  
*Source: own study.*

### 3.3. Quantity of the production batches.

In practice, different formulas for determining the size of a production batches are used, for example: the minimum variable cost, the minimum cost of the unit

or a specific share  $t_{pz}$  in  $t_c$ . The approach of the minimum unit cost of a product can't be directly attributed to the maximization of the use of available resources, i.e. the increase in productivity (8.9). All approaches are additionally determined by the times of completion of orders and ordered quantities and modified by information about inventory levels of materials and finished products as well as production and administration fixed costs. The analysis omits the most important element of forecasting and taking the risk of taking "shelf" production and determined time warnings due to delays in material supplies and possible failures [5]. In [1,2], an important possibility of division of the order into production batches with smaller quantities was taken into account, which despite the increase in labor intensity (greater share of  $t_{pz}$  time) significantly improves the use of work stands, and thus the productivity of operational programs, by optimizing the ordering of technological operations. Under given assumptions, the quantities  $J_j$  (5) of the total technological time of orders are known and the unit technological times of individual operations are known. The proposed formula does not take into account the decrease in costs due to deferred payments for materials, discounts related to the size of the order, market disturbances, frozen funds, etc., and as a function of the target, the minimum working time ( $K_{cj}$ ) in the production batch:

$$K_{rj} = \frac{t_{pz}}{n} + t_j \quad (8)$$

where:

- $K_{rj}$  – labor-consuming in the batch  $rbg$  (orders)  $J_j$  ;
- $n$  - the number of pieces in a lot;
- $t_{pz}$  - preparatory and completion time in  $rbg$ ;
- $t_j$  - unit work time in  $rbg$ .

The conversion into a financial measure can take place at unit costs (eg. in working hours) of a work stands. With such assumptions, the cost of manufacturing a production batch of  $n$  quantity products will be expressed by the formula:

$$K_{cj}(n, \mathfrak{S}_w) = n(K_m + K_{rj}) + nK_{sj} \quad (9)$$

where:

- $K_{cj}$  - total unit cost of a unit (natural or contractual) of the product in the production lot  $f(n, \mathfrak{S}_w)$ ;
- $K_{sj}$  - fixed costs, average for the settlement period related to the labor consumption to the unit of the considered product, but will be a function of the number of items  $f(n)$ ;



$K_m$  - costs of direct and indirect materials (assigned from the key) for the unit of the product under consideration, but there will be the function of the number of items  $n$ , and the function of the actual size of the operative program  $f(\mathcal{X}_v)$ .

The proposed approach to the productivity analysis gives the opportunity to link the unit cost of a contractual product or expressed in natural units with the productivity of the department or company. This doesn't allow a simple reference to the size of the production lot because the unit cost of the product will be associated with the use of resources.

#### **3.4. Accuracy and precise**

The achievement of a certain quality level in normal production conditions is assumed for the economic accuracy of a specific product characteristic. Multifactorial problem and difficult to define unequivocally. According to the proposal contained in [11], the average value of the cost of execution (normal) is proposed to take the cost with the accuracy of performance obtained in normal<sup>9</sup> (average) production conditions for specific stands, production departments or plant. The term "usual quality requirements" should be understood as generally accepted principles for the implementation of, e.g., free (non-tolerated) dimensions. A different problem of defining normal conditions, including related normal costs of technological operations carried out at individual work stands, is determining the use of resources at such a work. Increase of quality requirements will worsen the productivity of operative programs, and the adoption of works stands with lower accuracy, may improve productivity, but will usually worsen profitability. In the literature [8, 10] an expression is found determining the change in cost as a function of tolerance of characteristics (10, 11). In practice, the dependencies *Tolerance - Cost* are similar in nature, but require clarification in relation to specific departments, work-stands and employees experience. For CNN stands the extension of the technological time resulting from increased quality requirements results from the additional preparation of the machine, eg system calibration, heating and preparing stands, special preparation of tools, more machining passes, etc. With manual machines, unit times will be longer but there may be additional limitations for specific work stands and employees. There is a limit to the accuracy, below which the execution costs will not be further reduced, although productivity may increase. Dependencies (10, 11) are further modified by the risk of making non-compliant parts (improvement, repair, admission or necessity produce of a new one). In production practice, there is also the selection of work stations due to their condition and technical capabilities, the preparation of operators and their availability. Usually, the most accurate work

---

<sup>9</sup>The concept of normal operating conditions of an enterprise is defined differently in the Act of 29 September 1994 "On Accounting", Dz.U. U. 1994 No. 121 item 591, Chapter 4 Art.28. point 3 and in IAS.

stands are handled by more qualified employees and they are more expensive. Ultimately, the choice of a work stands (if such a possibility exists) will be determined by the cost of implementation and quality requirements and may cause additional limitation when the tasks of operational programs are optimally scheduling that is, deterioration of productivity.

$$K = a + c \frac{b}{T} \quad (10)$$

where:

$K$  - cost of production batch production;

$a$  - the cost of a stationary workstation;

$c$  - cost of  $Rbg$  of workstation performing work in normal production conditions;

$b$  - tolerance to carry out the production under normal production conditions;

$T$  - tolerance - accuracy.

$T$  tolerance consists of two elements:  $T_0$  - tolerance values which tightening will result in the lack of impossibility to maintain quality requirements and  $T_w$  - required tolerance for the execution of a specific technological operation (11):

$$T = T_0 + T_w \quad (11)$$

The boundary  $T$  values for a given technological operation will be:  $T_m$  - the value above which it can be assumed that the costs of the technological operation will no longer decrease and  $T_o$  - the minimum tolerance value possible to be achieved at the considered work stand and technical operation. Tightening tolerance may be replaced by an increase in labor consuming, which will be a disadvantage from the point of view of productivity.

### 3.5. Selection of a work stands

From the point of view of a better use of the available work stands, it is possible to analyze the choice of time based occupations in accordance with the formulas (12,13) combining the analyzed positions with the implementation time of individual technological operations:

$$T_c = t_j + \frac{t_{pz}}{n} = t_{ji} + \frac{t_{pzi}}{n} \quad (12)$$

$$n = \frac{t_{pzi} - t_{pz}}{t_j - t_{ji}} \quad (13)$$

where:

$i, j$  - technological times for available work stands.

When repeatability of order execution occurs, further retooling of work stations in the form of special instrumentation should be considered, and the

decision on its implementation will result from the conditions of profitability and productivity (in the sense of better use of the resources) in accordance with the simplified formula (14):

$$L_K = \frac{K}{(t_b - t_p)k_h} \quad (14)$$

where:

- $L_K$  - the critical number of parts (assemblies) which determines the use of special equipment;
- $t_b$  - unit specific time ( $t_{pz} + t_j$ ) of making parts without a special device. If there is a program implemented in production batches, it should be included in the value of  $t_{pz}$ . The calculation should be made for the normal technically justified conditions for the implementation of individual technological operations;
- $t_p$  - total unit time ( $tpz + t_j$ ) of making a part with an instrument (special devices) If it is a program implemented in production batches, this should be included in the value of  $t_{pz}$  ;
- $k_h$  - average cost of rbg on the considered workstation at the normal level of use of the work station;
- $K$  - cost of production and operation of the planned production device (s). Reference to larger or multi-annual programs.

Presented solutions in the field of technical and technological possibilities to improve productivity in the case of unit production and small-lot is not unambiguous, and the introduction of these technical and organizational solutions should be preceded by an economic analysis (profitability) and rational justification for their use, including, for example, risks of non-compliant products.

#### 4. Productivity of operative programs.

Typical preparation of operational programs of unit and small-lot production are based on balancing the available resources with the resources necessary to orders execution. With unit and small-series programs, optimization analyzes of materials cutting<sup>10</sup> or energy and so on are not rationally justified, hence the article focuses on using the available technological times at workplaces. The possibility of buying semi-prepared units from the required materials is observed, which is the case for companies offering materials with higher requirements. From the point of view of the profitability assessment of programs, more generalized criteria should be considered which include costs and risks of early start-up and delays in the execution of individual orders [5]. Optimization of the

---

<sup>10</sup>The time and costs of carrying out such analyzes exceed the effects of their introduction.

priorities of technological operations of operational programs can be carried out using various criteria. regardless of accepted or omitted restrictions. For simplicity, the article assumes that operational programs do not have priority orders or orders with the required completion dates. The equivalent criteria for the target function formulated in such a way which is maximum utilization will be [7]: minimization of the completion time of all orders  $\min C_{max}^{11}$ , minimization of time of work stands  $\min \sum I_k$ , and average utilization rates of available resources, understood here as the use of available time  $\max U$ - work at available work stands. Because the mentioned criteria are equivalent, the criterion  $\min C_{max}$  was used in the software used, with an additional analysis of the actual use of the available resources of global work time (for the department) and individual work stations [9]. The operational program can be represented by formulas (4) and (15.16):

$$\begin{aligned}
 a_{11}J_1 + a_{12}J_2 + \dots + a_{1i}J_j &\leq U_1; \\
 a_{21}J_1 + a_{22}J_2 + \dots + a_{2i}J_j &\leq U_2; \\
 &\dots \\
 a_{i1}J_1 + a_{i2}J_2 + \dots + a_{ij}J_j &\leq U_i;
 \end{aligned}
 \tag{15}$$

$$U = \sum_{i=1}^p U_i
 \tag{16}$$

where:

- $a_{ij}$  - technical production coefficients (they determine the amount of  $U_i$  resource necessary to execute the  $j$ -order product), eg. labor consuming;
- $J_j$  - successive orders of the production program (products)  $j = 1, \dots, m$ ;
- $U_i$  - resources  $i = 1, \dots, n$  understood here as availability of working positions.

The optimized ( $ST^{12}$ ) solution used, theoretically well-known, is not used in practice in practice, and its presentation is aimed at demonstrating the effects and validity of practical applications for the following reasons:

1. Gives the possibility of quantitative assessment of productivity at the stage of preparation and evaluation of the current implementation of operational programs, including possible deadlines for the execution of individual orders;
2. Allows for current and target modification of operative programs, taking into account the level of productivity and deadlines for completing orders;

---

<sup>11</sup>Markings as specified in [7].

<sup>12</sup>Tabu Search - metaheuristics by Fred Glover used to solve discrete optimization problems.

3. Allows for measurable, quantitative assessment of the parameters of the operational programs, including quantitative adjustments of renewable and non-renewable resources.

The IBM ILOG CP Optimizer solver was used to optimize the ordering of technological operations in specific orders of the operational program, but for simplicity it was assumed that there were no priority orders or deadlines. Evaluation and possibly "manual" corrections of bottlenecks of prepared operational programs can be introduced through modifications by two ways:

- modification of resources through overtime work;
- temporary use of work station stops by introducing orders to the "shelf" into the operational program.

After optimization of the program, adjustments of the resources being made are made and their use is improved by introducing, for example, orders into a "shelf"<sup>13</sup>. Minimizing the length of program execution time also gives the manager an insight into the deadlines and downtime of individual work stands as well as deadlines for the implementation of individual technological operations and deadlines for the completion of individual orders. The following information is available at this stage:

- the program is optimized for maximizing productivity;
- the manager has knowledge about threats and their sizes, eg delays;
- the manager has knowledge about stoppages at work positions and times of such stoppages;
- the manager has knowledge about the bottlenecks of the program and the time to take corrective actions to improve the program's productivity.

From the organizational point of view, these analyzes are in practice connected with additional limitations, eg timely completion of individual orders or the requirement to accelerate deadlines for their completion. In practice, individual orders can be divided into priority and special tasks (marked with weights) and execution of orders of a random nature. From the point of view of modeling the preparation and implementation of operational programs, these are issues in the areas of operational research and discrete programming of order processes. Due to the strong *NP*-difficulty and possible random changes, it is not rationally justified to use effective optimization algorithms. In [7], the equivalence of the criterion  $\min C_{max}$  (minimizing the completion time of all program tasks) and  $\min \Sigma I_k$  (minimizing the downtime of all work stations - resources participating in the operational program) and maximizing the utilization of resources  $\max. U$ -. They are equivalent because the optimal sequence of implementation of individual operations and orders for one of the

---

<sup>13</sup>Understood here as orders that can be used with low risk. More precisely, the risk that they will not be sold is low in relation to the cost of the post.

criteria is also the optimal order for the other listed criteria. The optimization analysis of the ordering of technological operations of individual operative program was carried out for the criterion of  $\min C_{max}$ , ie. maximum productivity.

Table 3.1. Presentation of program optimization results with the use of working time of positions in *Rbg.* and % utilization of the resources available. *Source: own study.*

Stand 1			Stand 2			Stand 5			Stand 6		
Ord.	Start	Stop	Ord.	Start	Stop	Ord.	Start	Stop	Ord.	Start	Stop
2	0	6	4	0	5	2	13	28	14	16	26
10	6	20	14	5	10	7	28	33	4	35	55
5	20	29	7	10	11	8	33	38	3	55	85
9	29	41	3	11	16	5	41	48	2	85	105
1	41	61	13	16	17	14	48	58	9	105	117
1	183	<b>183</b>	6	17	22	1	63	63	12	117	130
			11	22	23	3	138	168	4	135	215
			8	23	24	1	177	183	13	215	221
			12	24	<b>25</b>	1	183	193	6	221	241
						13	232	238	11	241	<b>254</b>
						11	303	<b>309</b>			
$\Sigma$ Rbg		<b>62</b>	$\Sigma$ Rbg		<b>25</b>	$\Sigma$ Rbg		<b>101</b>	$\Sigma$ Rbg		<b>215</b>
Wyk. w %		<b>38,8</b>	Wyk. w %		<b>15,63</b>	Wyk. w %		<b>63,13</b>	Wyk. w %		<b>134,38</b>

As an example, the optimization of the technological operations of the production program with 14 orders was carried out with the required total time of 1615 *Rbg* carried out on 14 workstations with a total available time of 2240 *Rbg*. For simplicity it was assumed that the duration of individual operations will be expressed in full hours. This gave an average use of the available working time of each position at the level of 72%. Even so, only 3 orders will be processed in the settlement period - 160 *Rbg*. Tables 3.1 and 3.2 present the results of calculations for selected orders and workstations. The results presented are the simplest example of scheduling. without time and priority restrictions, they give an overview of the problems faced by the companies in the processes of preparing and implementing operative programs. The dividend of larger orders for subcontracts with fewer pieces in a lot and different start-up dates can definitely improve the use of available resources. The division of orders into production batches has been discussed in more detail in [1, 2]. Such a solution will result in

an increase in total unit times, but will improve the use of available resources. The biggest problem is the lack of available, at an acceptable cost, programs enabling such optimization analyzes.

Table 3.2. Dates of completion of selected orders in *Rbg.* counted from the beginning of the operational program. *Source: own study.*

Order 1			Order 2			Order 4			Order 5		
Stan.	Start	Stop	Stan.	Start	Stop	Stan.	Start	Stop	Stan.	Start	Stop
1	41	61	1	0	6	2	0	5	1	20	29
3	63	63	3	6	13	4	5	35	4	35	41
5	63	63	5	13	28	6	35	55	5	41	48
7	63	70	6	85	105	9	55	85	7	48	56
9	169	177	9	118	133	7	85	135	8	56	59
5	177	183	10	133	141	6	135	215	4	60	80
1	183	183	11	160	190	10	215	255	9	85	90
5	183	193	12	190	233	11	255	325	10	90	114
7	193	203	13	233	241	13	325	345	11	114	122
8	203	215	14	241	<b>253</b>	14	345	<b>355</b>	13	122	126
12	233	237							14	126	<b>127</b>
13	241	243									
14	253	<b>254</b>									

## 5. Conclusions

From the analysis of available methods of improving productivity for the case of unit and low-volume production, the most effective is the application of discrete optimization of operational programs. Known and discussed above commonly used solutions to improve the productivity of operational programs from the technological, qualitative and organizational side have limited applications in the case of unit and small-lot production, also for rational reasons. The effective solution to improve the organization of production processes and to improve productivity is the application of discrete optimization of operative programs and the introduction of adjustments allowing for ad hoc and better use of the available resources. A serious limitation, even when applying the proposed solution, are market restrictions, which were not explicitly considered and which are of significant importance for this type of business entities [5]. The use of proposed solutions for the preparation of operational programs with currently available tools and software, including proprietary computer systems at the ERP level is not problem for companies with relatively small production programs.

The preparation of technologies at the mentioned level (labor consumption and materials) is fully sufficient to carry out such optimization and productivity analyzes. The presented proposal additionally gives the opportunity to evaluate deadlines, bottlenecks, and the use of individual positions, hence the possibility of taking earlier and ad hoc actions such as additional *Rbg.* or outsourced production. Optimization calculations and results presented even in a simplified form in Tab. 3.1 and Table 3.2 are a good tool for production management. The relatively short calculation time (for orders of around 50 and around 40 work stands) does not exceed several minutes, and allows you to make changes and corrections even during the current business day. The barrier is the price of solvers with such possibilities for commercial use, especially for this type of companies.

## References

- [1] Bożek A., Werner F., *Flexible job shop scheduling with lot streaming and subplot size optimisation*. International Journal of production Research, 11 Jul 2017.
- [2] Bożek A., Wysocki M., *Off-line and Dynamic Production scheduling – a comparative case study*. Management and Production Engineering Review. Vol. 7, No 1, March 2016.
- [3] Brzeziński M.: *Podstawy metodyczne projektowania rozruchu nowej produkcji*, PWN, Warszawa 1996.
- [4] Brzeziński M.: *Z badań nad zjawiskiem zapominania nawyków roboczych*, Prace Naukowe Politechniki Lubelskiej, 148, Lublin 1997.
- [5] Brzęczek J., *Poddostawca w warunkach produkcji małoseryjnej* Zeszyty Naukowe PŁ, Organizacja i Zarządzanie, Zeszyt nr. 54, Łódź 1913
- [6] Brzęczek J., *Organizacyjne aspekty przygotowania i realizacji produkcji małoseryjnej*. Zeszyty Naukowe Politechniki Rzeszowskiej nr 270 Mechanika z. 78 z 2009 r.
- [7] Grabowski J., Nowicki E., Smutnicki C., *Metoda blokowa w zagadnieniach szeregowania zadań*. Akademicka Oficyna Wydawnicza EXIT Warszawa 2003
- [8] Jeziński J., *Analiza tolerancji i niedokładności pomiarów w budowie maszyn*. WNT Warszawa 1983.
- [9] Kaczmarczyk W.: *Nowe kryterium oceny stopnia wykorzystania maszyn dla zadań szeregowania produkcji*, Zeszyty Naukowe Politechniki Śląskiej, seria Automatyka, z. 129, Gliwice 2000.
- [10] Sokołowski A. *Kurs technologii budowy maszyn* PWT Warszawa 1952.
- [11] Szadkowski J.: *Ekonomiczne i technologiczne przesłanki wyboru tolerancji w układach łańcuchów wymiarowych*, Zeszyty Naukowe Politechniki Krakowskiej, nr 4, Kraków 1969.



## Chapter 4.

Paweł FIGIEL<sup>1</sup>  
Anna BIEDUNKIEWICZ<sup>1</sup>  
Witold BIEDUNKIEWICZ<sup>1</sup>  
Dariusz GRZESIAK<sup>1</sup>  
Dariusz GRABIEC<sup>2</sup>

# COMPARISON OF THE PROPERTIES OF TITANIUM CARBIDE IN TITANIUM MATRIX NANOCOMPOSITES MANUFACTURED BY SLM AND SPS TECHNIQUE

### Abstract

Titanium is more resistant to corrosion, but has a lower strength than its alloys. The use of Ti and its alloys as construction materials in conditions of high friction and wear is limited due to their restricted tribological properties. Appropriate selection of hard ceramic particles introduced into the titanium matrix and its alloys is an effective way to increase their mechanical and wear properties. The paper presents the results of research on the properties of titanium matrix composites (TMCs) reinforced with non-oxide ceramic nanoparticles. The evaluated materials were manufactured by selective laser melting (SLM) and spark plasma sintering (SPS) techniques. Commercial titanium cp-Ti (grade 1) was used as a matrix and nanocrystalline TiC encapsulated in elemental carbon cages (denoted nc-TiC/C) was used as a reinforcing phase. Powder mixtures containing 0, 5, 10 and 20wt% of nc-TiC /C were prepared for SPS and SLM processes. The influence of the reinforcing phase on tribological and corrosion properties of TMCs (nc-TiC /C/Ti) composites produced in SPS and SLM processes was studied in aqueous 3wt% solution of sodium chloride. As reference materials cp-Ti and Ti6Al4V samples obtained in SLM and SPS consolidation processes were used. Corrosion parameters were determined using the Tafel method based on the results of potentiodynamic measurements from anode polarization curves. The properties of titanium composites manufactured with SPS and SLM techniques were compared. It was found that the composites' wear resistance improved significantly, and the corrosion resistance deteriorated with the increase of nc-TiC content in the titanium matrix.

### Keywords:

Titanium nanocomposites, SLM and SPS sintering techniques, nc-TiC/C

---

<sup>1</sup> Faculty of Mechanical Engineering and Mechatronics., West Pomeranian University of Technology, Szczecin, Piastow 19 Av. 70-310 Szczecin, Poland

<sup>2</sup> Metal Forming Institute, Jana Pawła II Av. 61-130 Poznan, Poland

\* e-mail: anna.biedunkiewicz@zut.edu.pl

## 1. Introduction

Since the discovery of titanium in 1791, it is an extremely desirable material in production. Currently, the aviation industry is the largest customer of titanium alloys. There are several titanium properties that make it well suited to the aviation industry: high strength to weight ratio, its corrosion resistance. The low elastic modulus of titanium means excellent elasticity and strong springing properties. This favors its use in various aircraft springs and valves, in which the module is half of that for the steel, but the strength is equivalent for steel, which allows the titanium spring to be half as large and heavy. This property is also beneficial for components that must absorb vibrations or work under dynamic loads. The fraction of titanium used on the global aviation market increases with each new generation of aircraft structures [1-6].

Pure commercial titanium is cheaper, generally more resistant to corrosion, but has lower strength than its alloys and is not suitable for heat treatment. The use of titanium and its alloys as construction materials under conditions of high friction and wear is limited due to adverse tribological properties. Nevertheless, proper selection of hard ceramic particles for the titanium and its alloys matrix proved to be an effective way to improve its wear resistance in the friction process and other mechanical properties [7,8]. The advantage of composite materials is that their individual components retain their properties as opposed to alloys. As a result, various combinations of properties, usually unattainable for alloys, can be obtained with composite materials by matching suitable matrix and reinforcement. In general, metal matrix composites are used in wear applications due to their high hardness while maintaining a reasonable level of ductility. The overall abrasion resistance comes from hard particles, while the increase in ductility comes from the transition metal matrix. Wear resistance is a key aspect in which the internal properties of metallic composites reinforced with ceramics can be used. Strengthening titanium with a ceramic phase also improves its thermomechanical properties [9]. To maximize interfacial bond strength in metal matrix composites (MMCs), it is necessary to promote wetting, control chemical interactions, and minimize oxide formation. Adequate and consistent bonding between the matrix and the particles is necessary to achieve maximum strength of the composites. Interfacial connection is possible, among others, thanks to the reactive consolidation of the composite, i.e. as a result of a chemical reaction between the matrix and the reinforcing phase occurring in the sintering process. Particles of the reinforcing phase and matrix material react to form a new compound or compounds at the interface. They are responsible for bonding efficiency and thus composite consolidation, strength, low porosity and corrosion resistance. This approach guarantees a thermodynamically stable composite with clean interfaces, well consolidated, with maximum strength at low and elevated temperatures and resistance to brittle fracture. Composites obtain their hardness

and strength due to strong chemical bonds as well as due to crystal structure and nano-size of phase components.

The addition of hard ceramic particles of nc-TiC in carbon cages to the matrix has proved to be an effective way to improve the properties of titanium. The aim of this study was to analyze the effect of bonding of nc-TiC/C and titanium matrix on morphology, corrosion resistance and mechanical properties, in order to create a unique composite using spark plasma sintering (SPS) and selective laser melting (SLM) techniques. The composites were tested for mechanical properties and corrosion resistance in NaCl solution at a concentration of 3wt% and compared. The study used spark plasma sintering (SPS) and selective laser melting (SLM) techniques. Plasma sintering (SPS) is a newly developed versatile technique for quick sintering of powder materials in minute intervals compared to several hours required for conventional sintering processes. SPS involves applying simultaneously pressure and current directly to powder materials. A high pulsed direct current is applied to the electrode, and microscopic electrical discharges in the empty spaces between the powder particles generate plasma, causing sintering. The main difference between SPS and other sintering methods is that in the SPS process both the matrix and the strengthening phase are directly heated by the heat released during this process, the so-called Joule's heat. The HP D 25-3 FCT System GmbH device was used during the study. Selective laser melting (SLM) is a technique that uses a laser beam to selectively melt a layer of metal or metal mixed with ceramic particles in form of a powder, layer by layer, to obtain a final component based on 3D computer-aided design (CAD) data. Due to the growing industry demand for the production of lightweight components with complex shapes, SLM is becoming attractive for the automotive and aviation industries, including the production of components from titanium and its alloys. The SLM system (MCP HEK Realizer II) consisted of a fiber laser Nd: YAG, an automatic powder layer feeder and an argon gas protection system to prevent oxidation of the material.

## **2. Materials and methods**

### **2.1. Preparation of nc-TiC/C/Ti composites**

In this work, cp-Ti (grade 1) titanium powder obtained by gas atomization at SLM Solutions GmbH was used as the starting material for the composite matrix. Cp-Ti powder particles had a spherical shape and the average particle size was about 100  $\mu\text{m}$  (Fig. 4.1a). The reinforcement, nanocrystalline nc-TiC/C powder (Fig. 4.1b) with an average crystallite size of 40 nm and about 3wt% elemental carbon content was obtained by non-hydrolytic sol-gel method (Fig. 4.1b). The synthesis process, structure and morphology of nc-TiC/C powder have been presented earlier [10].

Titanium and nc-TiC/C powders were ground in an argon atmosphere using a Pulverisette 4 (Fritsch GmbH) planetary mill using WC/Co milling balls in

a weight ratio of 10:1 relative to the powder. Mixtures of powders composed of 0, 5, 10 and 20wt% of TiC/C and titanium, respectively, were used for the sintering process.

The HP D 25-3 FCT System GmbH device was used for the spark plasma sintering (SPS) process. The following sintering process parameters were used: sintering temperature - 1300°C, heating rate - 400°C/min, sintering time - 2.5 min, press pressure - 50 MPa, vacuum level - 5 Pa. The samples obtained in the process were cylindrical with a diameter of 20 mm and a height of 10 mm.

Selective laser melting of the mixture of nc-TiC/C and Ti powders was performed using the SLM system (MCP HEK Realizer II) consisting of a fiber laser Nd: YAG, an automatic powder layer feeder and an argon protection system. The parameters of the SLM process have been described earlier [12]. The density of the obtained composite materials was measured in water using Archimedes's method.

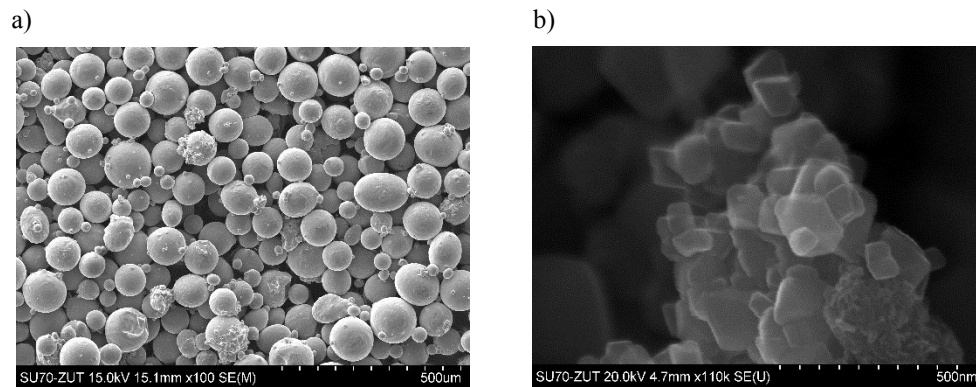


Fig. 4.1. Microstructure of the used powders: a) cp-Ti b) nc-TiC/C [11]

## 2.2. Structural and morphological characteristics of nc-TiC/C/Ti composites

The test samples were cut out, then polished using an ATM SAPHIR 550 grinder with an MD-Mezzo 220 disc and MD-Largo discs with the addition of a 9 µm diamond suspension. The finishing step was carried out on MD-Chem discs using Al<sub>2</sub>O<sub>3</sub> suspension with the addition of H<sub>2</sub>O<sub>2</sub>. In morphological tests, the second group of samples was grinded with 220 grit paper and electro-polished using Struers LectoPol-5 device with the following parameters: voltage 30-35 V, flow 16, time 20 s, surface area 1 cm<sup>2</sup> and Struers A3 electrolyte.

The average size of crystallites in composites was calculated by Scherrer and Debye-Hull methods. The crystallite size, phase composition, morphology and chemical composition of the composites were determined by the following techniques: X-ray diffraction (XRD) using the PANalytical PW3040 / 60 X'Pert

Pro apparatus equipped with Cu K $\alpha$  radiation, scanning electron microscopy (SEM) using the Hitachi SU-70 apparatus equipped with Thermo Fisher Noran 7 EDS microanalysis adapter.

### **2.3. Mechanical and tribocorrosion tests**

Vickers hardness (HV) measurements were carried out on a Leco LM247AT indenter at a load of 0.1 kG with an indentation time of 10 s. Tribocorrosion resistance of nanocomposites was tested using the "pin on disk" technique. Tests were carried out in dry air and in a 3wt% NaCl solution on a CSM tribometer (TRN model), using an alumina ball with a diameter of 6 mm, with the tested samples of nanocomposites acting as a disk.

Potentiodynamic polarization (LSV) measurements were performed at a scanning rate of 1 mV/s in the potential range -1.0 V to +1.0 V. For measurements, an Atlas-Sollich 9833 potentiometer was used in a three-electrode system. A calomel (reference) and graphite (auxiliary) electrode was used. The analysis of the results was carried out using AtlasLab software. All corrosion tests were carried out in a 3wt% NaCl solution.

Tribocorrosion (abrasive corrosion) properties of the composite samples were tested using the "ball-on-disk" method. Individual tests were carried out in a dry air atmosphere on a CSM tribometer (TRN model). An alumina ball with a diameter of 6 mm was in contact with the rotating disk of the tested composite material. A load of 1 and 3 N was applied, which corresponded to a sliding distance of 500 m. Before each test, the samples and the balls were ultrasonically rinsed in acetone. The standard deviation did not exceed 10%. The DEKTAK 6M profilometer (Veeco) was used to estimate volume loss (V) and wear coefficient (K).

### **3. Results and discussion**

X-ray diffractograms used to analyze the phase composition of composites and to determine the average size of TiC crystallites are presented in Figures 4.2, 4.3 and 4.4. Figure 4.2 presents a diffraction pattern of a powder containing TiC nanocrystallites in elemental carbon cages. The wide interference reflection corresponding to the angular position  $2\theta=25.34^\circ$  corresponds to graphite (002), while the other five reflections correspond to the position  $2\theta$   $36.21^\circ$  (111),  $42.06^\circ$  (200),  $60.99^\circ$  (220),  $73.04^\circ$  (311) and  $76.86^\circ$  (222) can be well assigned to TiC (ICDD 00-031-1400) [13]. Figure 4.3 presents a comparison of diffraction patterns of composites obtained by the SPS method, and Figure 4.4 a comparison of diffraction patterns of composites obtained by the SLM method, containing 0, 5, 10, 20wt% of nc-TiC/C respectively.

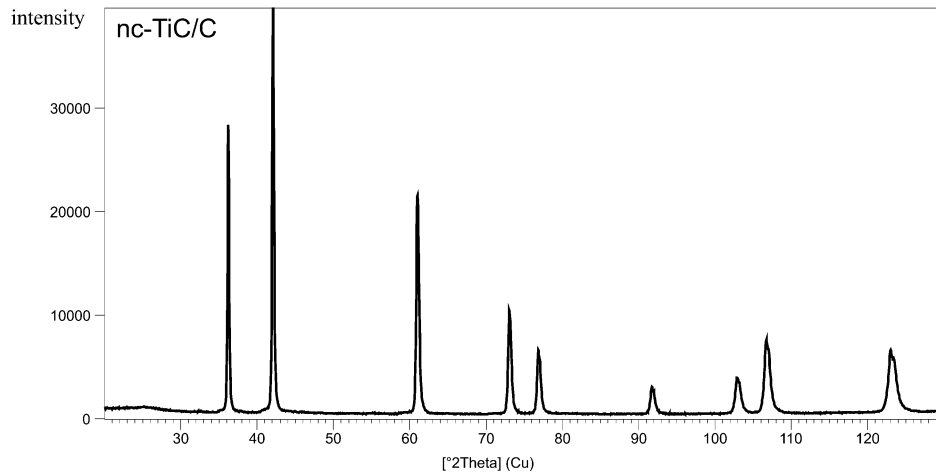


Fig. 4.2. X-ray diffraction pattern of titanium carbide in a carbon cage nc-TiC/C

Analysis of the results of the X-ray diffraction method showed changes in the intensity distribution of titanium interference reflections with an increase in the nc-TiC/C fraction in composites obtained by the SPS method. The proportions between the intensities of interference reflections  $I_{101}/I_{002}$  of the reference titanium sample and the composites differed compared to the proportions resulting from the JCPDS pattern file. This means that in all the samples, both reference and composites, the Ti phase showed texture. During the sintering process by SPS, the orientation of titanium crystallites changed from anisotropic to random. The largest deviations from random orientation were found in the reference titanium sample obtained with the SPS method. At the same time, with the increase in the TiC/C content in composites, the ratio of the intensity of interference reflection of titanium  $I_{101}/I_{002}$  in composites decreased, suggesting a change in the orientation of titanium crystallites from anisotropic to random. This phenomenon was not observed in materials consolidated by SLM technique; in all samples the orientation of Ti crystallites was random. In all tested composites, no changes in the orientation of nc-TiC crystallites were observed when changing their content in titanium matrix. Crystallites of nc-TiC in all composites were characterized by anisotropy, as evidenced by the higher intensity of the  $d_{111}$  reflex compared to the  $d_{200}$  reflex.

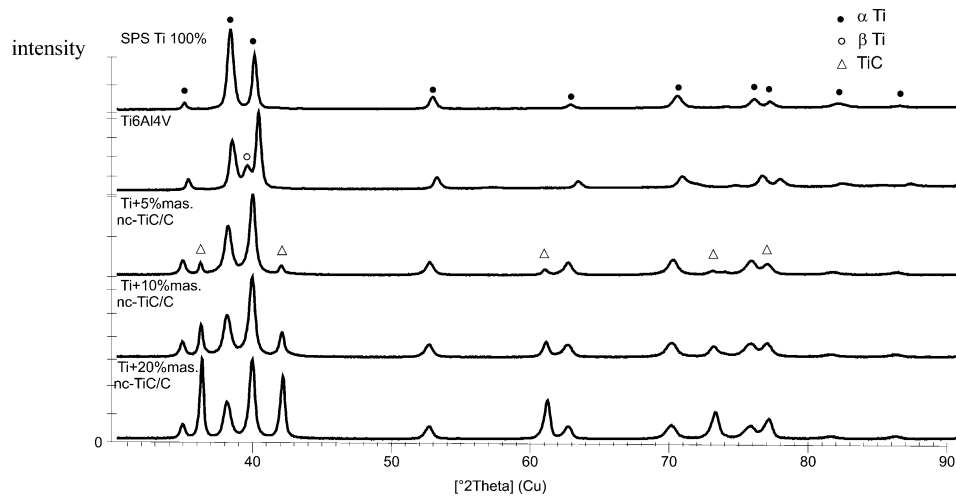


Fig. 4.3. Comparison of XRD diffractograms of nc-TiC/C/Ti composites and reference samples of Ti and Ti6Al4V alloy manufactured using the SPS technique

The microstructure images in Figures 4.5 and 4.6 show the distribution of the nc-TiC reinforcing phase in a titanium matrix. In composites manufactured by SPS technique the reinforcing phase was located in the inter-crystalline areas of the composite structure (Fig. 4.5a, b). Microscopic observations and comparison of the most intense interference reflections of titanium and TiC on X-ray diffraction patterns of nc-TiC/Ti composites revealed that the fraction of intercrystalline areas in relation to titanium matrix areas increased with the increase in the nc-TiC/C content, and the size of areas occupied by titanium crystallites decreased as a result of the reaction:  $\text{Ti} + \text{C} \rightarrow \text{TiC}$ .

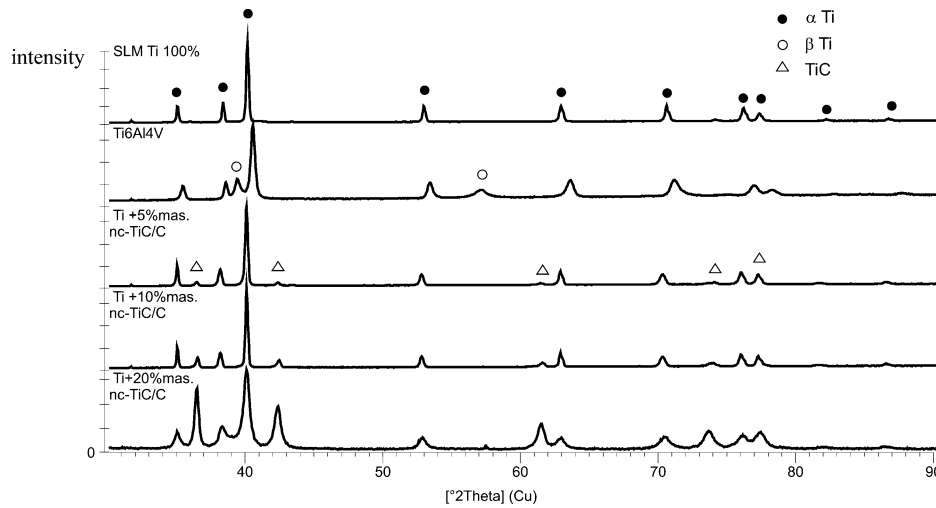


Fig. 4.4. Comparison of XRD diffractograms of nc-TiC/C/Ti composites and reference samples of Ti and Ti6Al4V alloy manufactured using the SLM technique

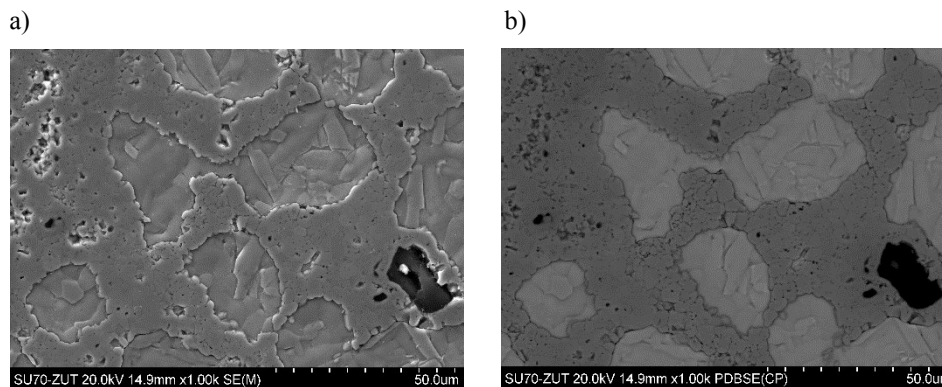


Fig. 4.5. Images of SE (a) and PDBSE (b) SEM of the surface microstructure of Ti + 20wt% nc-TiC/C composite produced by the SPS technique (black spots - pores)

Small and evenly distributed pores of irregular shape were observed on the surface of the tested composites. Incidentally larger pores appeared, about a dozen micrometers in size, in composites with the highest content of reinforcing phase, i.e. on the surface of Ti + 20wt% nc-TiC/C composites manufactured by the SPS technique (Fig. 4.5a, b).



Figure 4.6 presents the image of the microstructure of the Ti + 10wt% nc-TiC/C composite manufactured by SLM technique. Microscopic observations showed that titanium carbide was dispersed evenly in the titanium matrix, which was characterized by dendritic morphology, nc-TiC aggregates were less frequently observed (Fig. 4.6 a). These observations were confirmed by the results of the chemical composition analysis carried out by the EDS method in points 1-9 (Fig. 4.6 b, c).

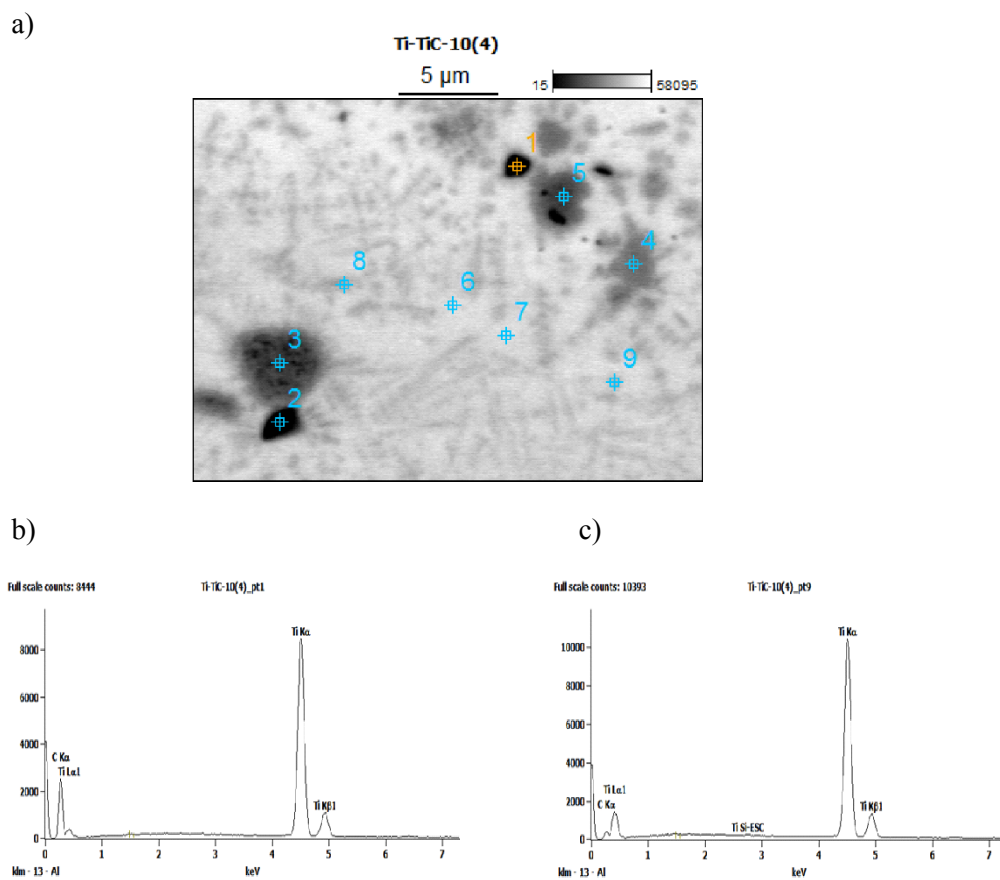


Fig. 4.6. a) SEM image of the surface microstructure of Ti + 10wt% nc-TiC/C composite manufactured by SLM technique, b) and c), EDS spectra at points 1 and 9, respectively

Figure 4.7 presents diagrams illustrating the density changes of composites manufactured using SLM (Fig. 4.7a) and SPS techniques (Fig. 4.7b). Density of

the TiC reinforcement (4.92 g/cm<sup>3</sup>) compared to that of pure titanium (4.507 g/cm<sup>3</sup>) is similar, therefore changes in the relative density of the composites should be attributed to their porosity. Composites obtained with the SPS technique had the highest densities. In both cases, the density decreased as the content of the reinforcing phase increased.

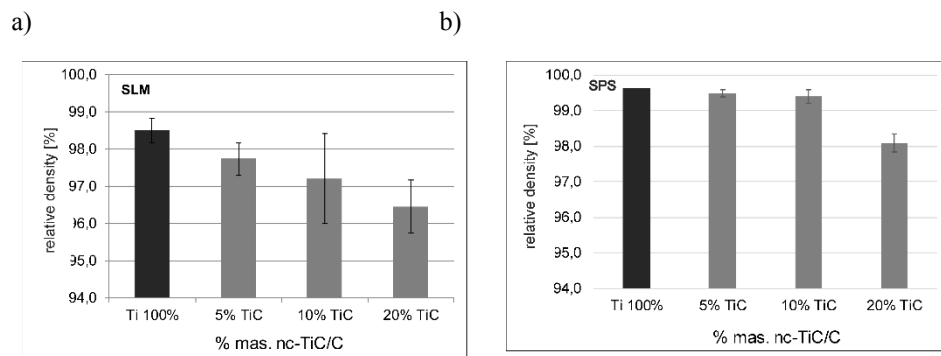


Fig. 4.7. Comparison of the results of density measurements of composites obtained using a) SLM and b) SPS techniques

The hardness of the composites increased along with the increase in the content of the nc-TiC reinforcing phase. In the case of Ti + 20wt% nc-TiC/C composites produced by SLM and SPS techniques hardness was three times higher compared to metallic titanium (Fig. 4.8).

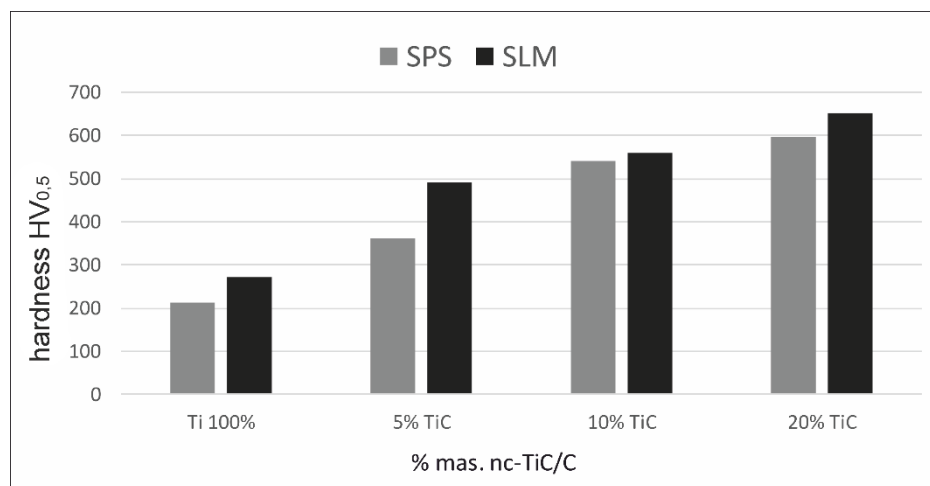


Fig. 4.8. Comparison of Vickers hardness measurement results

Tribocorrosion resistance of nanocomposites was tested using the "pin on disk" technique. The volume loss (V) and wear coefficient (K) of titanium and composites were estimated. Tests carried out in dry air showed an increase in resistance to abrasive wear along with an increase in the content of the reinforcing phase for both types of composites, i.e. those obtained with the SPS technique and SLM technique (Fig. 4.9a, b). Ti + 20wt% nc-TiC/C composites were characterized by the highest tribocorrosion resistance. Tribocorrosion (abrasive corrosion) resistance of SPS composites evaluated in a 3wt% NaCl solution increased monotonically with the increase of the reinforcing phase content (Fig. 4.10b). Tribocorrosion (abrasive corrosion) resistance of SLM composites has deteriorated compared to metallic titanium in the case of Ti + 5 and 10wt% nc-TiC/C composites (Fig. 4.10a). Improvement of resistance was found only in the case of Ti + 20wt% nc-TiC/C composite. Observed decrease in abrasion-corrosion resistance of Ti + 5 and 10wt% nc-TiC/C composites probably results from susceptibility to intergranular corrosion.

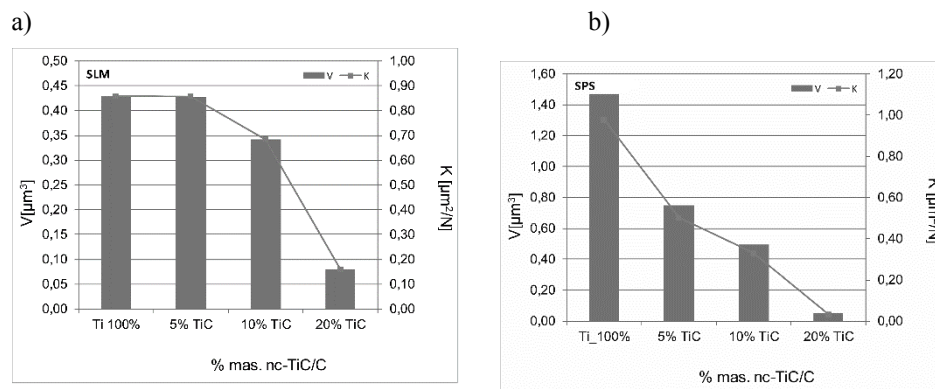


Fig. 4.9. Comparison of tribological test results of composites manufactured using a) SLM and b) SPS techniques

Potentiodynamic polarization measurements were performed at a scanning rate of 1 mV/s in the potential range -1.0 V to +1.0 V. All corrosion tests were carried out in a 3wt% NaCl solution. The comparison of polarizing curves is presented in Figure 4.11a, b. Corrosion parameters of titanium and the composites determined by the Tafel method are listed in Table 4.1.

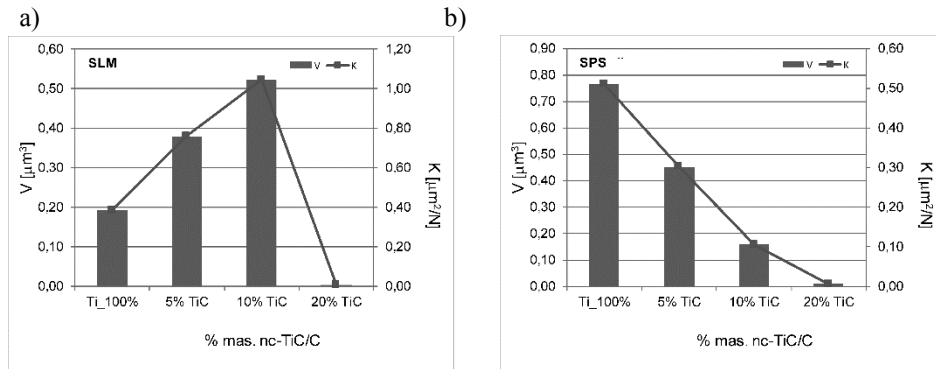


Fig. 4.10. Comparison of tribocorrosion test results of composites manufactured using a) SLM and b) SPS techniques

Test results showed that polarization curves of SLM composites were shifted in the cathodic region of lower potential values compared to the polarization curve for titanium. The course of anode sections suggests that the durability of passive layers produced on titanium and its composites is comparable. Composites were characterized by higher values of corrosion potentials and higher values of density of corrosion current along with the increase of the content of nc-TiC in the titanium matrix. Composites consolidated by SLM technique compared to metallic titanium are characterized by inferior corrosion resistance in the environment of a 3wt% NaCl solution.

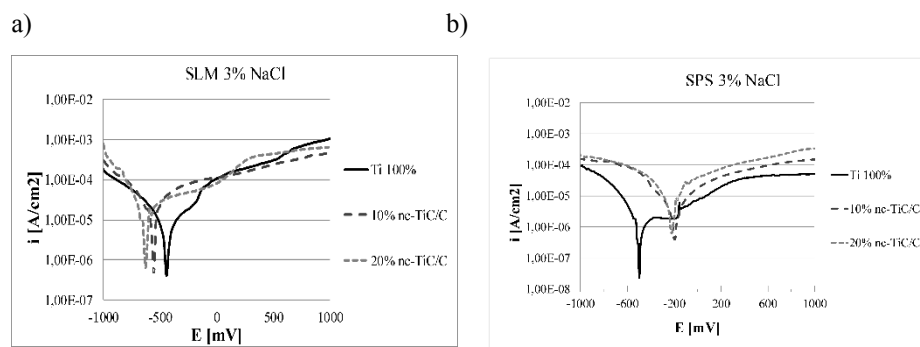


Fig. 4.11. Comparison of test results of anode polarization curves in a 3wt% NaCl solution of composites manufactured using a) SLM and b) SPS techniques

Table. 4.1. Corrosion parameters of titanium and the composites in 3wt% NaCl solution

process	samples	$E_{\text{corr.}}$ , [V]	$i_{\text{corr.}}$ [A/dm <sup>2</sup> ]
SPS	Ti 100%	-497	$1,15 \cdot 10^{-6}$
	10% nc-TiC/C	-195	$21,48 \cdot 10^{-6}$
	20% nc-TiC/C	-224	$22,78 \cdot 10^{-6}$
SLM	Ti 100%	-447	$3,15 \cdot 10^{-6}$
	10% nc-TiC/C	-583	$12,50 \cdot 10^{-6}$
	20% nc-TiC/C	-639	$13,62 \cdot 10^{-6}$

The polarization curves of the composites manufactured by SPS technique were shifted in the anodic region, i.e. higher potential values, compared to the polarization curve for titanium. The anode section curves suggest that the durability of the passive layers produced on titanium is higher compared to the passive layers on the composites. The composites are characterized by higher values of corrosion potential compared to the corrosion potential of titanium and lower values of density of corrosion current compared to the corrosion potential of titanium. The highest value of corrosion potential was noted for Ti + 10wt% nc-TiC/C composite.

The measure of corrosion resistance is the density of corrosion current, so in conclusion it should be stated that the highest corrosion resistance in an environment of 3wt% NaCl solution was exhibited by titanium manufactured by SPS technique, followed by titanium manufactured by SLM technique. Among all the tested nc-TiC/C/Ti composites, Ti + 10wt% nc-TiC/C composite produced by SLM technique is characterized by the highest resistance.

## References

- [1] <http://c.ymcdn.com/sites/www.titanium.org/resource/resmgr/Docs/TiUltimate.pdf>; accessed: 03.04.2018r.
- [2] Takahashi N., Sato T., Nakatsuka S., Fujiwara K., Yokozekii K., Titanium metal matrix composite development for commercial aircraft landing gear structure, Proceedings of 28<sup>th</sup> International Congress of The Aeronautical Sciences 2012, Brisbane, Australia, (2012) [http://www.icas.org/ICAS\\_ARCHIVE/ICAS2012/PAPERS/037.PDF](http://www.icas.org/ICAS_ARCHIVE/ICAS2012/PAPERS/037.PDF); 16.01.2017

- [3] Boyer R.R.(1996). An overview on the use of titanium in the aerospace industry. *Materials Science and Engineering A213*, 103-114. DOI: 10.1016/0921-5093(96)10233-1
- [4] <https://tmstitanium.com/titanium-and-the-aerospace-industry/>; 07.05.2019
- [5] <https://industrialtalks.wordpress.com/2012/12/12/why-titanium-is-used-in-the-aircraft-industry/> 23.04.2019
- [6] <https://continentalsteel.com/titanium/applications/>25.04.2019
- [7] Van Acker K., Vanhoyweghen D., Persoons R., Vangrunderbeek J. (2005)., Influence of tungsten carbide particle size and distribution on the wear resistance of laser clad WC/Ni coatings. *Wear* 258 (1-4), 194-202. DOI:10.1016/j.wear.2004.09.041
- [8] Cavanaugh D. T. (2015). Evaluation of titanium carbide metal matrix composites deposited via laser cladding, *Graduate Theses and Dissertations* Iowa State University, Ames, USA
- [9] Poletti C., Balog M., Schubert T., Liedtke V., Edtmaier C. (2008)., Production of titanium matrix composites reinforced with SiC particles. *Compos. Sci. Technol.* **68** (9), 2171-2177. DOI:10.1016/j.compscitech.2008.03.018
- [10] Biedunkiewicz A. (2011), Manufacturing of ceramic nanomaterials in Ti–Si–C–N system by sol–gel method. *J. Sol-Gel Sci. Technol.* 59:448–455 DOI 10.1007/s10971-010-2237-2
- [11] Figiel P., Grabiec D., Biedunkiewicz A., Biedunkiewicz W., Kochmański P., Wróbel R. (2018). Microstructural, corrosion and abrasive characteristics of titanium matrix composites, *Arch. Metall. Mater.* 63(4), 2049-2057. DOI: 10.24425/amm.2018.125142
- [12] Biedunkiewicz A., Figiel P., Grzesiak D., Biedunkiewicz W., Patent P. 407355 (2014).
- [13] Christensen A.N. (1975), A Neutron Diffraction Investigation on Single Crystals of Titanium Carbide, Titanium Nitride, and Zirconium Nitride. *Acta Chem.Scand.Ser.A*. 29, 563-564. DOI: 10.3891/acta.chem.scand.29a-0563

## Chapter 5.

Aleksandra KRUK<sup>1\*</sup>  
Sławomir ZIMOWSKI<sup>2</sup>  
Tomasz MOSKALEWICZ<sup>1</sup>

# PEEK AND PEEK-BASED COATINGS FOR IMPROVEMENT OF THE TI-6AL-4V ALLOY'S TRIBOLOGICAL PROPERTIES

### Abstract

Ti-6Al-4V is the most frequently used titanium alloy, mainly as a construction material. However, despite its favorable mechanical properties, low density and good electrochemical corrosion resistance, it has poor tribological properties, which significantly limits its applications. To improve the tribological properties of this alloy, in the present work we fabricate polymeric PEEK 708 as well as composite Si<sub>3</sub>N<sub>4</sub>/PEEK 708 and PTFE/PEEK 708 coatings by electrophoretic deposition (EPD) and heat treatment. The chemical composition of the suspensions used for EPD was determined as well as the mechanisms of particle EPD. PEEK coatings were successfully deposited from pure ethanol. In the case of composite coatings, it was necessary to add cationic polyelectrolyte, which increased the suspension's stability and enabled coating deposition. To obtain homogeneous coatings, the EPD parameters, such as voltage and time, were selected. As-deposited coatings were heat treated above the PEEK 708 melting point and cooled with a furnace. Such treatment densifies the coatings and increases their adhesion to the substrate. PEEK 708 and Si<sub>3</sub>N<sub>4</sub>/PEEK 708 coatings exhibited very good scratch resistance, higher than the low-friction PTFE/PEEK 708 coating. The tribological properties of the coated and uncoated alloy were investigated in cooperation with an Al<sub>2</sub>O<sub>3</sub> ball in dry contact at room temperature using the ball-on-disc system. It was found that all coatings reduced the friction coefficient of the alloy from 0.70 to 0.10, 0.26 and 0.27 for the PTFE/PEEK 708, Si<sub>3</sub>N<sub>4</sub>/PEEK 708 and PEEK708 coated alloy. In addition, all coatings significantly increased the titanium alloy's wear resistance. The lowest wear rate was exhibited by the PTFE/PEEK 708 composite coating.

**Keywords:** Tribological properties, electrophoretic deposition, Ti-6Al-4V alloy, polyetheretherketone, composite coatings

---

<sup>1</sup> Faculty of Metals Engineering and Industrial Computer Science, AGH University of Science and Technology, Czarnowiejska 66, 30-054 Kraków, Poland

<sup>2</sup> Faculty of Mechanical Engineering and Robotics, AGH University of Science and Technology, Mickiewicza Av. 30, 30-059 Kraków, Poland

\*e-mail: kruk@agh.edu.pl

## 1. Introduction

The Ti-6Al-4V alloy belongs to the group of important construction materials and is also the most widespread two-phase ( $\alpha + \beta$ ) titanium alloy [1]. More than half of the commercial applications of all titanium alloys are carried out with the use of this alloy, due to two main reasons; (i) firstly, because of its very good combination of properties, low density and Young's modulus, good electrochemical corrosion resistance and a favorable balance between strength and plasticity [2, 3], and (ii) secondly, it is now the most intensively investigated and developed titanium alloy [4]. Despite its numerous advantages, this material exhibits poor tribological properties, a high coefficient of friction (COF) as well as low abrasion and wear resistance [5]. These drawbacks significantly limit the possible use of this material in applications with exposure to wear and friction. In order to improve the tribological properties, and consequently to increase the potential applications, surface treatment is often used, including the deposition of polymer or composite polymer-based coatings.

Thermoplastic polymers are a group of materials combining many positive features, such as low density and high mechanical strength [6]. Therefore, they are increasingly used as coatings to enhance the usable properties of metals. One representative polymer is polyetheretherketone (PEEK), which is often referred to as a high-performance engineering material [7]. It is a semi-crystalline polymer with a linear structure and its melting point is in the range of 330 - 385 °C. PEEK is an easy-to-mold material with good thermal stability and chemical resistance. It also has good mechanical and tribological properties [8, 9]. All these features make it a good material for individual applications as well as a matrix of composites for various purposes [10, 11]. The fabrication of composite materials with the PEEK matrix seems to be an ideal solution which enables the favorable mechanical properties of polymer to be combined with the high hardness of ceramic particles. In this work, we decided to use silicon nitride ( $\text{Si}_3\text{N}_4$ ) nanoparticles as a reinforcement phase to increase the abrasion and wear resistance of PEEK as well as polytetrafluoroethylene (PTFE) particles to reduce the COF of PEEK.  $\text{Si}_3\text{N}_4$  is a ceramic material exhibiting very good mechanical and tribological properties, such as high hardness, high mechanical strength and high abrasion resistance [12, 13]. Therefore, it is used as a reinforcing phase for polymeric materials, for example polyethylene [14] or polypropylene [15]. PTFE is a well-known and widely used synthetic fluoropolymer. It is characterized by the lowest friction coefficient among all plastics, as well as high chemical and thermal resistance [16 – 18].

One of the versatile methods that allows coatings to be produced, especially polymeric or composite, including PEEK and PEEK-based ones, is electrophoretic deposition (EPD). It is an electrochemical process that allows coatings of various thicknesses to be deposited on conductive substrates [19]. The process takes place in two stages. In the first stage, the charged particles move



towards the oppositely charged electrode under an electric field, while in the second, they deposit on the electrode and form a coating [20]. This method does not require the use of expensive equipment and offers many possibilities of combining various materials, thus the interest in it is fast growing [21]. In recent years, PEEK and PEEK-based coatings have also been deposited by other methods, for example, thermal spraying [22] and printing technology [8].

In the last years, EPD has been mostly used for the deposition of polymer-based coatings without heat treatment, mainly for medical applications [23 – 25]. However, these coatings wear gradually and the protection is usually lost. An outcome of this work is the development of composite polymer-based coatings densified by heat treatment and modified by the addition of hard Si<sub>3</sub>N<sub>4</sub> nanoparticles or PTFE lubricant to improve the tribological properties of titanium alloy. The main aim of the present work was to fabricate polymeric PEEK 708, composite Si<sub>3</sub>N<sub>4</sub>/PEEK 708 and PTFE/PEEK 708 coatings on Ti-6Al-4V alloy substrates by the use of EPD and heat treatment, as well as to investigate their scratch resistance and to determine their impact on the tribological properties of the alloy.

## 2. Materials and methods

The inspiration for the research was to improve the tribological properties of the titanium alloy, especially for applications in mechanical engineering. The authors postulate that PEEK 708, Si<sub>3</sub>N<sub>4</sub>/PEEK 708 and PTFE/PEEK 708 coatings fabricated by EPD and heat treatment will enhance the tribological properties of the Ti-6Al-4V alloy during friction in dry sliding conditions at room temperature.

The two-phase ( $\alpha + \beta$ ) Ti-6Al-4V alloy was used as a substrate material for coating deposition. The alloy was delivered in the form of a rod by BÖHLER Edelstahl GmbH, Germany, in the hot rolled and annealed condition, 750 °C/2 hours. The samples for deposition were in the form of discs with a diameter of 22 mm and a thickness of 3 mm. The samples were ground with successively finer grit of sandpaper up to 3000-grit and polished with the standard colloidal SiO<sub>2</sub> suspension (OP-S, 0.04  $\mu$ m) of Struers. Directly before deposition, samples were washed with distilled water and technical ethanol.

PEEK 708, Si<sub>3</sub>N<sub>4</sub> and PTFE powders were used as coating components. The PEEK powder was delivered by Victrex Europa GmbH (Germany). Its melting point is 374 °C, the glass transition temperature is 157 °C and the density is 1.32 g/cm<sup>3</sup>. Si<sub>3</sub>N<sub>4</sub> powder with a density of 3.4 g/cm<sup>3</sup> was delivered by Nanostructured & Amorphous Materials, Inc. (USA). PTFE powder was delivered by Micro Powders, Inc. (USA) and its density is 2.2 g/cm<sup>3</sup>. Chitosan with a medium molecular weight and deacetylation degree about 75 - 85% delivered by Sigma-Aldrich (Poland) was used as a cationic polyelectrolyte in suspensions for EPD.

In order to deposit coatings, three suspensions with the following chemical compositions were prepared; (i) 1.5 g of PEEK 708 in 50 ml of ethanol, (ii) 0.02

g of  $\text{Si}_3\text{N}_4$  and 1.5 g of PEEK 708 in 50 ml of a dispersion medium containing 75 vol% of ethanol and 25 vol% of chitosan polyelectrolyte, (iii) 0.1 g of PTFE and 1.5 g of PEEK 708 in 50 ml of a dispersion medium containing 75 vol% of ethanol and 25 vol% of chitosan polyelectrolyte. The chemical composition of the chitosan polyelectrolyte was 0.5 g/l of chitosan, 1% acetic acid and distilled water. All the suspensions were mixed for 10 minutes with a magnetic stirrer and ultrasonically dispersed for 15 minutes to eliminate the agglomerates. The zeta potential of particles as a function of the suspension's pH was measured using a Zetasizer Nano ZS 90 from Malvern Instruments Ltd., (UK). The pH value was measured using the ELMETRON CPC-505 pH meter (Poland). The measurements were carried out in both dispersion media, pure ethanol and in ethanol with the addition of chitosan polyelectrolyte. The pH was lowered with citric acid and increased with sodium hydroxide.

Electrophoretic deposition was carried out in a standard two-electrode system using the EX752M PSU Multi-mode power supply (UK). A constant voltage in the range of 10 - 90 V with 10 V changes and constant times of 20, 40 and 90 s were applied for the PEEK 708, PTFE/PEEK 708 and  $\text{Si}_3\text{N}_4$ /PEEK 708 coatings, respectively. AISI316L (X2CrNiMo17-12-2) austenitic stainless steel was used as the counter electrode. The distance between the electrodes was 10 mm for PEEK 708 coatings and 15 mm for composite coatings. In the case of polymer coatings, the titanium alloy sample was an anode, while in the case of composite coatings, cathodic electrophoretic deposition was used.

Heat treatment of the PEEK 708 and  $\text{Si}_3\text{N}_4$ /PEEK 708 coatings was carried out in a Carbolite-Gero LHT 4/30 laboratory oven, (UK). The following temperatures and heating times of 380 °C for 20 min and 390 °C for 40 min were applied for the PEEK 708 and  $\text{Si}_3\text{N}_4$ /PEEK 708 coated alloy, respectively. Heat treatment of the PTFE/PEEK 708 coated alloy was carried out at 450 °C for 20 min in an LHT 08/18 furnace, Nabertherm GmbH (Germany). The cooling rate was 2 °C/min (with a furnace) in all treatments.

Microstructure characterization of the as-deposited and heat-treated coatings was carried out with the use of an FEI Nova NanoSEM 450 (USA) scanning electron microscope (SEM) and JEOL JEM-2010 ARP (Japan) transmission electron microscope (TEM). Phase identification was performed by X-ray diffraction (XRD) in grazing incidence XRD (GIXRD) geometry using a Panalytical Empyrean DY1061 diffractometer (Netherlands). The chemical composition was determined by energy dispersive X-ray spectroscopy (EDS) microanalysis. The thickness of the coatings was measured using the contact profilometry method on a trace length of 15 mm with a CSM Instruments Micro-Combi Tester (MCT) (Switzerland).

The microhardness and Young's modulus of the substrate and coatings were investigated by the instrumental indentation method using a Vickers indenter. A load of 200 mN, a loading and unloading speed of 400 mN/min as well as

a load of 100 mN and a speed of 200 mN/min were used for measurements of the substrate and the coatings, respectively. In all cases, the dwell time at the maximum load was 15 seconds. Each measurement was repeated at least six times, changing the place of indentation on the sample by several hundred micrometers each time to remove the influence of the previous measurement.

The adherence of the coatings to the substrate was determined in micro scratch tests with the use of a Micro-Combi-Tester (MCT) device and a Rockwell C diamond stylus with a radius of 200  $\mu\text{m}$ . The scratch track length was 5 mm, and the speed of the table with the fixed sample was constant, 5 mm/min. During the test, the load increased linearly from 0.01 to 30 N. The critical loads  $L_{C1}$  (corresponding to cohesive cracks) and  $L_{C2}$  (corresponding to adhesive failure) were determined. The coating surface after the scratch test was observed by a light microscope (LM) and SEM.

Tribological tests were performed in dry sliding conditions at room temperature (RT) using an equipped ball-on-disc tribometer (ITeE Radom, Poland). The  $\text{Al}_2\text{O}_3$  ball with a diameter of 6 mm, used as a counter body, was washed in acetone and, after drying, placed in a holder and then pressed with a constant force to the rotating sample. The tests were carried out with the following parameters of normal load 5 N, sliding speed 0.05 m/s, friction radius 3 mm and sliding distance 2000 m. The friction coefficient was determined based on the following equation:

$$\text{COF} = \frac{F_t}{F_n}$$

where:  $F_t$  is friction force and  $F_n$  is normal load.

The specific wear rate was determined from the following equation:

$$W_v = \frac{V}{F_n \cdot s}$$

where  $V$  is the volume of removed material,  $F_n$  - normal force, and  $s$  - sliding distance.

### **3. Results and discussion**

#### **3.1. Electrophoretic deposition of coatings**

The microstructure of the alloy used as a substrate material for coating deposition was investigated previously by Moskalewicz et al. [26]. The PEEK 708 and  $\text{Si}_3\text{N}_4$  powders used for coating deposition exhibited an amorphous structure and their size was in the ranges of 2 – 15  $\mu\text{m}$  and 5 – 30 nm, respectively.

PTFE powder had a crystalline structure and particle size in the range of 3 – 8  $\mu\text{m}$ .

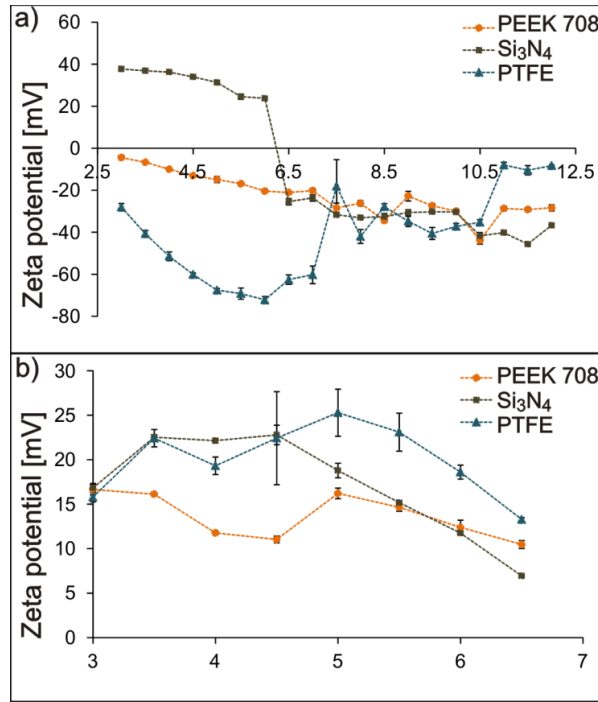


Fig. 5.1. Zeta potential of the PEEK 708, Si<sub>3</sub>N<sub>4</sub> and PTFE particles in pure ethanol (a) and in the ethanol-based suspension with the addition of chitosan polyelectrolyte (b) as a function of pH

PEEK 708 coatings were successfully deposited on the titanium alloy from pure ethanol, similarly to that in other previous works [9, 27 – 29], in which PEEK coatings were deposited mainly on stainless steel substrates. In the case of composite coatings, it was necessary to add polyelectrolyte to increase the stability of the suspensions, and thus enable deposition. Chitosan cationic polyelectrolyte was selected. The mechanism of its interaction with PEEK particles was described by Luo and Zhitomirsky [30]. The stability of suspensions can be inferred from the zeta potential value [31]. Therefore, measurements of the zeta potential of particles in suspensions was performed, and the results are shown in Figure 5.1. Zeta potential was measured for suspensions with a pH range of 3 - 12 and 3 - 6.5 for pure ethanol and for suspensions with chitosan polyelectrolyte, respectively. Above pH = 6, the precipitation of chitosan is usually observed [32]. The results showed that the zeta potential of PEEK and

PTFE particles in pure ethanol is negative throughout the entire pH range measured. In the case of  $\text{Si}_3\text{N}_4$  particles, an isoelectric point was observed at  $\text{pH} = 5$ . Below this point, the potential was negative, while it was positive above it. There is an opinion in the literature that the suspension is stable if the zeta potential is equal or higher than  $\pm 30$  mV [33]. Despite the relatively high zeta potential values of both  $\text{Si}_3\text{N}_4$  and PTFE particles, deposition from pure ethanol was not observed. The addition of chitosan polyelectrolyte caused a change in the surface potential of PEEK and PTFE particles from negative to positive. The highest values of zeta potential were  $16.65 \pm 0.59$  mV for  $\text{pH} = 3$ ,  $22.78 \pm 1.09$  mV for  $\text{pH} = 4.5$  and  $25.28 \pm 2.64$  mV for  $\text{pH} = 5$  for PEEK 708,  $\text{Si}_3\text{N}_4$  and PTFE particles, respectively. Although the particle potential values were lower compared to those in pure ethanol, the suspensions were stable enough to deposit coatings. Based on zeta potential measurements, a deposition mechanism for composite coatings has been proposed. Chitosan molecules and chains adsorb on PEEK and PTFE microparticles as well as  $\text{Si}_3\text{N}_4$  nanoparticles, preventing the formation of agglomerates and changing the surface charge, and consequently enable effective particle co-deposition. A schematic drawing of the co-deposition mechanism of the  $\text{Si}_3\text{N}_4$  and PEEK 708 as well as PTFE and PEEK 708 particles is shown in Figure 5.2.

To obtain homogeneous coatings, the EPD parameters, such as voltage and time, were selected in an experimental approach. It was observed that the as-deposited PEEK 708 coatings were uniform over a wide voltage range of 50 - 90 V. After EPD with a voltage lower than 50 V, the coatings were inhomogeneous and did not cover the substrate completely. After EPD with a voltage higher than 90 V, the coatings were thick, but not equal in thickness. A coating deposited at 70 V during 20 s was selected for further investigations. For the  $\text{Si}_3\text{N}_4$ /PEEK 708 coatings, deposition was not observed below the voltage of 40 V, and the coatings exhibited homogeneity after deposition in the voltage range of 60 - 90 V. However, below 80 V they were relatively thin. Thus, the coating deposited at 90 V during 90 s was selected for further research. PTFE/PEEK 708 coatings were macroscopically homogeneous after deposition with the voltage range of 70 - 90 V. They were thin and not uniform after deposition with the voltage range of 30 - 60 V, and below 30 V there was no deposition. The coating deposited at 90 V during 40 s was chosen for further investigations.

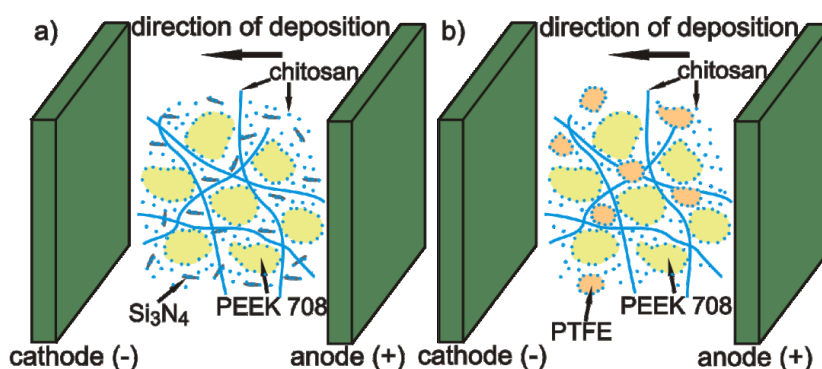


Fig. 5.2. Schematic drawings of the co-deposition mechanism for the  $\text{Si}_3\text{N}_4$  and PEEK 708 particles (a) and PTFE and PEEK 708 particles (b) from the ethanol-based suspension containing chitosan polyelectrolyte

### 3. 2. Microstructure of as-deposited and heat treated coatings

The microstructure of the as-deposited coatings was observed with the use of a scanning electron microscope. The results showed that all the as-deposited coatings were homogeneous and the particles were quite evenly distributed on the alloy's surface (Fig. 5.3). In the case of the  $\text{Si}_3\text{N}_4$ /PEEK 708 coating, separate  $\text{Si}_3\text{N}_4$  particles and their small agglomerates adsorbed to large polymer particles (Fig. 5.3b). Heat treatment of the coatings was conducted in order to densify them and increase their mechanical properties as well as adhesion to the substrate. XRD investigations showed that heating above the melting point of PEEK 708 and cooling with a furnace resulted in the formation of a semi-crystalline structure of PEEK in pure PEEK 708 and  $\text{Si}_3\text{N}_4$ /PEEK 708 coatings. A representative X-ray diffraction pattern for a pure PEEK 708 coating is shown in Figure 5.4 (marked with the letter A). It was difficult to identify the presence of  $\text{Si}_3\text{N}_4$  in the pattern due to the fact that the main diffraction peak coincides with the main diffraction peak from the polymer. However, TEM-EDS microanalysis enabled clearly distinguish both phases. In contrast, the PTFE/PEEK 708 coating after heat treatment exhibited an amorphous structure (Fig. 5.4, marked with the letter B). Such a polymer structure after heating and cooling with a furnace is unexpected, because a semi-crystalline structure is usually obtained after similar heat treatment, as was observed in our previous studies [29, 34, 35]. This phenomenon requires a more detailed explanation and will be the subject of further investigations.

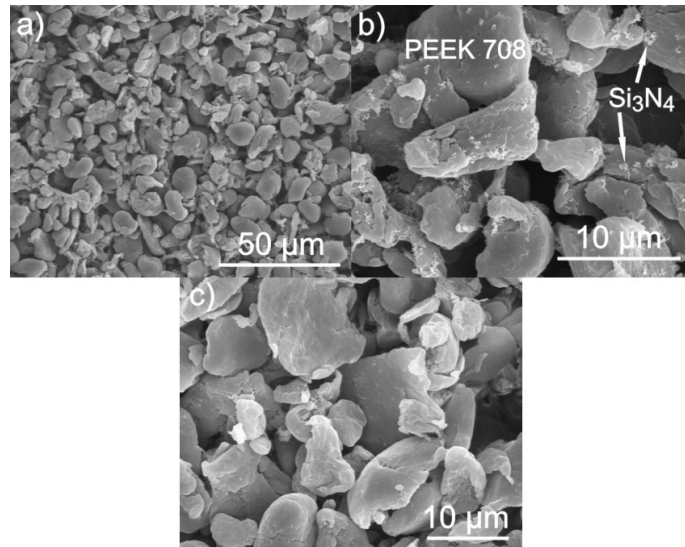


Fig. 5.3. Morphology of as-deposited PEEK 708 (a),  $\text{Si}_3\text{N}_4$ /PEEK 708 (b) and PTFE/PEEK 708 (c) coatings, SEM plan-view specimens

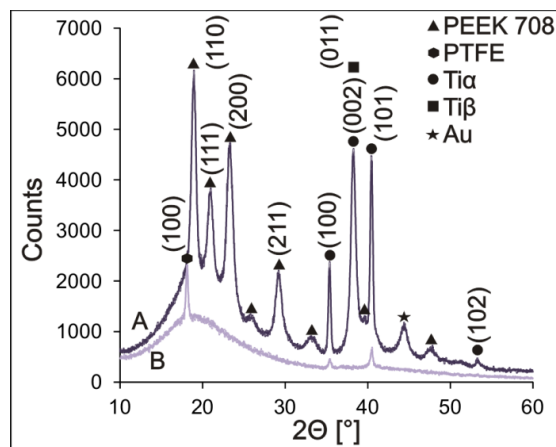


Fig. 5.4. GIXRD patterns of the PEEK 708 (A) and PTFE/PEEK 708 (B) coatings after heat treatment. The patterns were performed at a low incidence angle of  $3^\circ$  for PEEK 708 and  $1^\circ$  for PTFE/PEEK 708 coatings. Au comes from the prior evaporation of samples for SEM investigations

The microstructure of coatings after heat treatment is shown in Figure 5.5. In all cases, it can be seen that the coatings were compact without any cracks and voids. High surface development can be observed in the PEEK 708 coating due

to a typical spherulitic structure with a spherulite size up to 4  $\mu\text{m}$  (Fig. 5.5a). The  $\text{Si}_3\text{N}_4$ /PEEK 708 coating also showed relatively large surface development, mainly due to the high degree of open porosity (Fig. 5.5b). The PTFE/PEEK 708 coating was characterized by the smoothest and most uniform surface, probably due to its completely amorphous structure (Fig. 5.5c). The thickness of coatings was approx. 65  $\mu\text{m}$ , 90  $\mu\text{m}$  and 45  $\mu\text{m}$  for the PEEK 708,  $\text{Si}_3\text{N}_4$ /PEEK 708 and PTFE/PEEK 708 coatings, respectively.

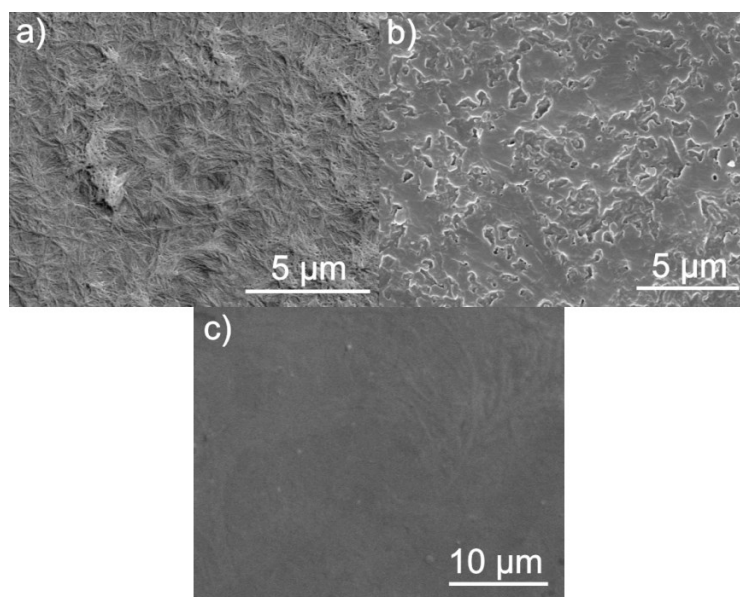


Fig. 5.5. Microstructure of the heat treated PEEK 708 (a),  $\text{Si}_3\text{N}_4$ /PEEK 708 (b) and PTFE/PEEK 708 (c) coatings, SEM plan-view specimens

### 3. 3. Scratch resistance, micro-mechanical and tribological properties

Based on the scratch track observation, penetration depth and friction force changes, as well as acoustic emission signal, no adhesive failure was found in either the PEEK 708 or  $\text{Si}_3\text{N}_4$ / PEEK 708 coatings up to a load of 30 N, the maximum load of the MCT (Fig. 5.6b). This indicates the very good adhesion of both coatings to the titanium alloy substrate. The PTFE/PEEK 708 coating showed a significantly lower scratch resistance, as evidenced by its delamination under the load  $L_{C2} = 23$  N (Fig. 5.6c). It was observed during the test that large fragments of the coating were removed and easily detached from the substrate. This process was accompanied by a clear acoustic emission signal, which indicates a kind of brittleness, but also the stiffness of the coating. However, no cohesive cracks were evident in this coating, as the cracks were probably just before delamination. In the PEEK 708 coating, the first cohesive cracks were



observed at the load  $L_{C1} = 23$  N (Fig. 5.6a), which resulted mainly from its large plastic deformation. The  $\text{Si}_3\text{N}_4/\text{PEEK 708}$  coating revealed the highest scratch resistance, despite the presence of open porosity. During the tests, no cohesive cracks were observed in the scratch tracks or their borders.

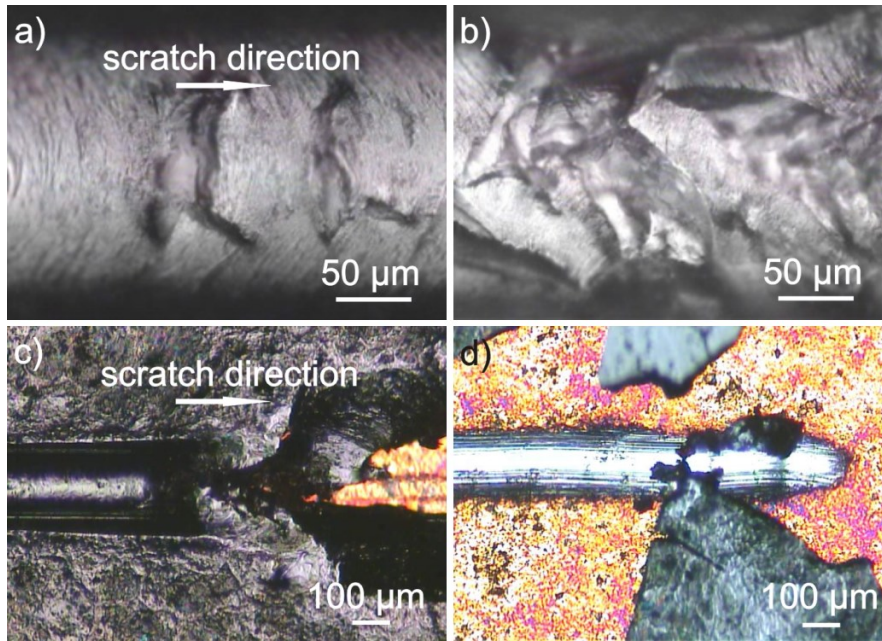


Fig. 5.6. LM images of the scratch track in the PEEK 708 coating under the load  $L_{C1} = 23$  N (a) and 30 N (b) as well as in the PTFE/PEEK 708 coating under the load  $L_{C2} = 23$  N (c) and 30 N (d)

Table 5.1. Hardness ( $H_{IT}$ ), Young's modulus ( $E_{IT}$ ) and the penetration depth of the indenter ( $h_{max}$ ) at the maximum load  $P_{max}$

Material	$P_{max}$ [mN]	$h_{max}$ [nm]	$H_{IT}$ [GPa]	$E_{IT}$ [GPa]
PEEK 708 coating	100	$3980 \pm 98$	$0.32 \pm 0.02$	$5.9 \pm 0.2$
$\text{Si}_3\text{N}_4/\text{PEEK 708}$ coating	100	$4269 \pm 68$	$0.30 \pm 0.02$	$5.4 \pm 0.2$
PTFE/PEEK 708 coating	100	$5236 \pm 1062$	$0.20 \pm 0.08$	$4.3 \pm 1.6$
Ti-6Al-4V alloy	200	$1596 \pm 86$	$3.63 \pm 0.30$	$120 \pm 14$

The results of micro-mechanical tests (Table 5.1) indicate that the PEEK 708 coating has comparable microhardness and elastic modulus to the  $\text{Si}_3\text{N}_4/\text{PEEK 708}$  coating, which might be due to the presence of open porosity in the composite

coating. Significantly lower values of microhardness and modulus of elasticity were measured for the PTFE/PEEK 708 coating. This may be related to its amorphous structure, which is significantly less resistant to the indenter. In addition, attention should be paid to the large spread of results from the average value for this coating, which may indicate that the microstructure is not homogeneous and that PTFE agglomerates are present in the coating.

Nevertheless, the PTFE/PEEK 708 coating exhibited the lowest coefficient of friction of all the investigated coatings, as expected, and its value was 0.1 (Fig. 5.7). The COF for the PEEK 708 and  $\text{Si}_3\text{N}_4$ /PEEK 708 coatings were higher, close to each other and equaled 0.27 and 0.26, respectively. Therefore, all the coatings significantly reduced the COF of the Ti-6Al-4V alloy, which was high and equaled 0.70.

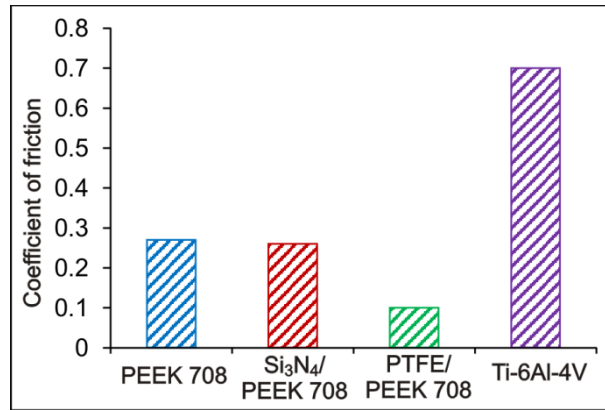


Fig. 5.7. Mean values of the COF of the PEEK 708,  $\text{Si}_3\text{N}_4$ /PEEK 708 and PTFE/PEEK 708 coated alloy as well as the uncoated Ti-6Al-4V alloy

The wear mechanism of the PEEK 708 coating was mainly abrasive. Wear debris was located mostly outside the wear track and slightly in the contact zone. Its wear rate was the highest of all the investigated coatings (Fig. 5.8). The specific wear rate of the composite  $\text{Si}_3\text{N}_4$ /PEEK 708 coating was much lower than the pure polymer coating, and no cracks or discontinuities were observed in the wear track. Interestingly, the PTFE/PEEK 708 coating, which was supposed to be low-friction only, also had the lowest wear rate. It exhibits very low resistance to motion due to the presence of sliding PTFE particles and high resistance to wear despite its brittleness. In spite of the different values of specific wear rates, and consequently different wear resistance, none of the coatings were totally abraded from the substrate during the tests. It should be concluded that all the coatings provide good protection of the titanium alloy substrate against

tribological wear and significantly reduce its volume wear rate, which was very high and equal to  $720 \cdot 10^{-6} \text{ mm}^3/\text{Nm}$ .

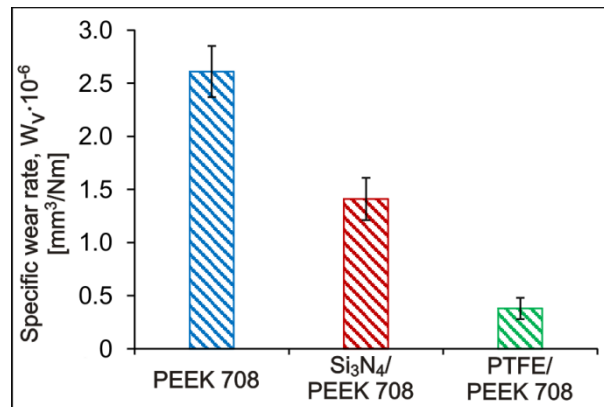


Fig. 5.8. Specific wear rate of the PEEK 708,  $\text{Si}_3\text{N}_4/\text{PEEK 708}$  and PTFE/PEEK 708 coatings on the Ti-6Al-4V alloy substrate

#### 4. Conclusions

1. Electrophoretic deposition and post-deposition heat treatment allowed homogeneous and dense polymeric PEEK 708 as well as composite  $\text{Si}_3\text{N}_4/\text{PEEK 708}$  and PTFE/PEEK 708 coatings to be produced. The addition of chitosan polyelectrolyte to suspensions changed the surface potential of all the particles used for EPD, increased their stability and, as a consequence, enabled the co-deposition of polymer and ceramic particles.

2. PEEK 708 and  $\text{Si}_3\text{N}_4/\text{PEEK 708}$  coatings exhibited very good scratch resistance and higher hardness, in contrast to the PTFE/PEEK 708 coating.

3. All of the coatings significantly reduced the coefficient of friction and increased the wear resistance of the Ti-6Al-4V alloy/coating system. The most significant enhancement of the tribological properties was shown by the PTFE/PEEK 708 coating.

The obtained investigation results clearly indicate that the fabrication of PEEK and PEEK-based coatings definitely improves the tribological properties of the titanium alloy/coating system, which significantly expands the possibilities of its applications. Further research will involve the investigation of tribological properties at the elevated temperatures of 150 and 260 °C, in order to determine the influence of increasing the friction pair temperature on the wear and friction behavior of the coated alloy.

## Acknowledgments

This work was supported by the National Science Centre, Poland (decision no DEC-2016/21/B/ST8/00238).

The authors appreciate the valuable contribution of DSc A. Kopia for XRD investigation and Dr Ł. Cieniek for SEM investigation.

## References

- [1] Muhammad M., Masoomi M., Torries B., Shamsaei N., Haghshenas M., (2018) Depth-sensing time-dependent response of additively manufactured Ti-6Al-4V alloy, *Addit. Manuf.* 24, 37 - 46,
- [2] Ye X., Wang L., Tse Z. T. H., Tang G., Song G., (2015) Effects of high-energy electro-pulsing treatment on microstructure, mechanical properties and corrosion behavior of Ti-6Al-4V alloy, *Mater. Sci. Eng. C*, 49, 851 - 860
- [3] Oh I.-H., Nomura N., Masahashi N., Hanada S., (2003) Mechanical properties of porous titanium compacts prepared by powder sintering, *Scr. Mater.*, 49 (12), 1197 - 1202
- [4] Peters M., Hemptenmacher J., Kumpfert J., Leyens C., (2003) Titanium and Titanium Alloys, *Fundamentals and Applications*, Chapter 1 - Structure and Properties of Titanium and Titanium Alloys
- [5] Niu Q. L., Zheng X. H., Ming W. W., Chen M., (2013) Friction and Wear Performance of Titanium Alloys against Tungsten Carbide under Dry Sliding and Water Lubrication, *Tribol. Trans.*, 56 (1), 101 - 108
- [6] Zhang G., Yu H., Zhang C., Liao H., Coddet C., (2008) Temperature dependence of the tribological mechanisms of amorphous PEEK (polyetheretherketone) under dry sliding conditions, *Acta Mater.*, 56 (10), 2182 - 2190
- [7] Kadiyala A. K., Bijwe J., Kalappa P., (2018) Investigations on influence of nano and micron sized particles of SiC on performance properties of PEEK coatings, *Surf. Coat. Technol.*, 334, 124 - 133
- [8] Zhang G., Li W. -Y., Cherigui M., Zhang C., Liao H., Bordes J. -M., Coddet C., (2007) Structures and tribological performances of PEEK (poly-ether-ether-ketone)-based coatings designed for tribological application, *Prog. Org. Coat.*, 60 (1), 39 - 44
- [9] Wang C., Ma J., Cheng W., (2003) Formation of polyetheretherketone polymer coating by electrophoretic deposition method, *Surf. Coat. Technol.*, 173 (2 - 3), 271 - 275
- [10] Lu Z. P., Friedrich K., (1995) On sliding friction and wear of PEEK and its composites, *Wear*, 183, 624 - 631
- [11] Li E. Z., Guo W. L., Wang H. D., Xu B. S., Liu X. T., (2013) Research on tribological behavior of PEEK and glass fiber reinforced PEEK composite, *Phys. Procedia*, 50, 453 - 460
- [12] Xia R., Zhang Y., Zhu Q., Qian J., Dong Q., Li F., (2008) Surface Modification of Nano-Sized Silicon Nitride with BA-MAA-AN Tercopolymer, *J. Appl. Polym. Sci.*, 107, 562 - 570
- [13] Golla B. R., Ko J. W., Kim J. M., Kim H. D., (2014) Effect of particle size and oxygen content of Si on processing, microstructure and thermal conductivity of sintered reaction bonded Si<sub>3</sub>N<sub>4</sub>, *J. Alloys Compd.*, 595, 60 - 66
- [14] Deepthi M. V., Sailaja R. R. N., Sampathkumaran P., Seetharamu S., Vynatheya S., (2014) High density polyethylene and silane treated silicon nitride nanocomposites using

- high-density polyethylene functionalized with maleate ester: Mechanical, tribological and thermal properties, *Mater. Des.*, 56, 685 - 695
- [15] Hao W., Yang W., Cai H., Huang Y., (2010) Non-isothermal crystallization kinetics of polypropylene/silicon nitride nanocomposites, *Polym. Test.*, 29 (4), 527 - 533
- [16] Liu Y., Xu N., Wang Y., Yao Y., Xiao H., Jia J., Lv H., Zhang D., (2019) Preparation and tribological properties of hybrid PTFE/Kevlar fabric self-lubricating composites, *Surf. Coat. Technol.*, 361, 196 - 205
- [17] Jia Y., Wan H., Chen L., Zhou H., Chen J., (2016) Effects of nano-LaF<sub>3</sub> on the friction and wear behaviors of PTFE-based bonded solid lubricating coatings under different lubrication conditions, *Appl. Surf. Sci.*, 382, 73 - 79
- [18] Khedkar J., Negulescu I., Meletis E. I., (2002) Sliding wear behavior of PTFE composites, *Wear*, 252 (5 - 6), 361 - 369
- [19] Besra L., Liu M., (2007) A review on fundamentals and applications of electrophoretic deposition (EPD), *Prog. Mater. Sci.*, 52 (1), 1 - 61
- [20] Corni I., Ryan M. P., Boccaccini A. R., (2008) Electrophoretic deposition: From traditional ceramics to nanotechnology, *J. Eur. Ceram. Soc.*, 28 (7), 1353 - 1367
- [21] Clavijo S., Membrives F., Boccaccini A. R., Santillán M. J., (2014) Characterization of polyetheretherketone particle suspensions for electrophoretic deposition, *J. Appl. Polym. Sci.*, 131 (20), 2 - 7
- [22] Patel K., Doyle C. S., Yonekura D., James B. J., (2010) Effect of surface roughness parameters on thermally sprayed PEEK coatings, *Surf. Coat. Technol.*, 204, 3567 - 3572
- [23] Jugowiec D., Łukaszczyk A., Cieniek Ł., Kot M., Reczyńska K., Cholewa-Kowalska K., Pamuła E., Moskalewicz T., (2017) Electrophoretic deposition and characterization of composite chitosan-based coatings incorporating bioglass and sol-gel glass particles on the Ti-13Nb-13Zr alloy, *Surf. Coat. Technol.*, 319, 33 - 46
- [24] Jugowiec D., Łukaszczyk A., Cieniek Ł., Kowalski K., Rumian Ł., Pietryga K., Kot M., Pamuła E., Moskalewicz T., (2017) Influence of the electrophoretic deposition route on the microstructure and properties of nano-hydroxyapatite/chitosan coatings on the Ti-13Nb-13Zr alloy, *Surf. Coat. Technol.*, 324, 64 - 79
- [25] Clavijo S., Membrives F., Quiroga G., Boccaccini A. R., Santillán M. J., (2016) Electrophoretic deposition of chitosan/Bioglass® and chitosan/Bioglass®/TiO<sub>2</sub> composite coatings for bioimplants, *Ceram. Int.*, 42 (12), 14206 - 14213
- [26] Moskalewicz T., Wendler B., Zimowski S., Dubiel B., Czyska-Filemonowicz A., (2010) Microstructure, micro-mechanical and tribological properties of the nc-WC/a-C nanocomposite coatings magnetron sputtered on non-hardened and oxygen hardened Ti-6Al-4V alloy, *Surf. Coat. Technol.*, 205 (7), 2668 - 2677
- [27] Ma J., Wang C., Liang C. H., (2007) Colloidal and electrophoretic behavior of polymer particulates in suspension, *Mater. Sci. Eng. C*, 27 (4), 886 - 889
- [28] Corni I., Neumann N., Eifler D., Boccaccini A. R., (2008) Polyetheretherketone (PEEK) coatings on stainless steel by electrophoretic deposition, *Adv. Eng. Mater.*, 10 (6), 559 - 564
- [29] Sak A., Moskalewicz T., Zimowski S., Cieniek Ł., Dubiel B., Radziszewska A., Kot M., Łukaszczyk A., (2016) Influence of polyetheretherketone coatings on the Ti-13Nb-13Zr titanium alloy's bio-tribological properties and corrosion resistance, *Mater. Sci. Eng. C*, 63, 52 - 61
- [30] Luo D., Zhitomirsky I., (2015) Electrophoretic Deposition of Polyetheretherketone Composites, Containing Huntite and Alumina Platelets, *JES*, 162 (11), 3057 - 3062

- [31] Ammam M., (2012) Electrophoretic deposition under modulated electric fields: A review, *RSC Adv.*, 2 (20), 7633 - 7646
- [32] Chung Y. C., Tsai C. F., Li C. F., (2006) Preparation and characterization of water-soluble chitosan produced by Maillard reaction, *Fish. Sci.*, 72, 1096 - 1103
- [33] Kervadec D., Haussonne J. -M., Vallar S., El Fallah J., Houivet D., (1999) Oxide slurries stability and powders dispersion: optimization with zeta potential and rheological measurements, *J. Eur. Ceram. Soc.*, 19 (6 - 7), 1017 - 1021
- [34] Moskalewicz T., Zych A., Kruk A., Kopia A., Zimowski S., Sitarz M., Cieniek Ł., (2018) Electrophoretic deposition and microstructure development of  $\text{Si}_3\text{N}_4$ /polyetheretherketone coatings on titanium alloy, *Surf. Coat. Technol.*, 350, 633 - 647
- [35] Moskalewicz T., Zimowski S., Zych A., Łukaszczyk A., Reczyńska K., Pamuła E., (2018) Electrophoretic Deposition, Microstructure and Selected Properties of Composite Alumina/Polyetheretherketone Coatings on the Ti-13Nb-13Zr Alloy, *JES* 165 (3), 116 - 128

## **Streszczenie**

MATERIAL, TECHNOLOGIES, CONSTRUCTIONS: "Special purpose processes" to monografia składająca się z pięciu rozdziałów o tematyce dotyczącej procesów wytwarzania. Pierwszy rozdział porusza zagadnienia procesu laserowego cięcia tworzyw sztucznych akrylu, polipropylenu w zależności od mocy lasera i grubości materiału. W drugim rozdziale przedstawiono wpływ właściwości narzędzi tnących, na jakość powierzchni stali P6M5. W rozdziale trzecim omówiono proces opracowania przygotowania i aktualizacji programów z zakresu produkcji a przede wszystkim wpływu tych zmian. Możliwość zmiany i optymalizacji programów obsługujących procesy produkcyjne w trakcie produkcji pozwala na zwiększenie produktywności. Rozdział czwarty to porównanie właściwości nanokompozytów na osnowie tytanu wykonanych z zastosowaniem procesów wytwarzania SLM i SPS. Określono właściwości powstałych warstw: twardość, zużycie, odporność korozyjną. Piąty rozdział dotyczy zagadnień zwiększania odporności na zużycie warstw wykonanych na bazie stopu tytanu. Określono właściwości warstw z zastosowaniem techniki zarysowania scratch oraz twardość, moduł Younga i penetrację wglębniaka.

## **Abstract**

MATERIAL, TECHNOLOGIES, CONSTRUCTIONS: "Special purpose processes" is a monograph consisting of five chapters on manufacturing processes. The first chapter deals with the process of laser cutting of acrylic and polypropylene plastic materials depending on the laser power and material thickness. The second chapter presents the influence of the cutting tool properties on the surface quality of P6M5 steel. The third chapter discusses the process of preparing and updating the programs in the scope of production and essentially the influence of these changes. The possibility of programs changes and optimizations supporting the production processes during the production process allows to increase the productivity. Chapter four compares the properties of titanium-based nanocomposites made with the use of SLM and SPS manufacturing processes. The properties of the following layers were determined as: hardness, wear and tear, corrosion resistance. The fifth chapter concerns the issues of increasing the wear resistance of the layers made on the titanium-based alloy. The properties of the layers were determined using the scratch technique, hardness, Young's modulus and indenter penetration.